Best Practices in Plant Fluorescence Imaging and Reporting - A Primer

Author Names and Affiliations:

Kirk J. Czymmek, Advanced Bioimaging Laboratory, Donald Danforth Plant Science Center, 975 N Warson Road, St. Louis, MO 63132 USA

Yoselin Benitez-Alfonso, Centre for Plant Sciences, School of Biology, University of Leeds, Leeds, LS2 9JT. United Kingdom

Tessa Burch-Smith, Donald Danforth Plant Science Center, 975 N Warson Road, St. Louis, MO 63132 USA

Luigi F. Di Costanzo, Department of Agricultural Sciences, University of Naples Federico II, 80055 Portici, Italy

Georgia Drakakaki, Department of Plant Sciences, University of California Davis, Davis, CA 95616, USA

Michelle Facette, Department of Biology, University of Massachusetts, Amherst, 221 N. Pleasant St., Amherst, MA 01003 USA

Daniel Kierzkowski, Département de Sciences Biologiques, Institut de Recherche en Biologie Végétale, Université de Montréal, 4101 Sherbrooke St E, Montréal, QC H1X 2B2, Canada

Anastasiya Klebanovych, Advanced Bioimaging Laboratory, Donald Danforth Plant Science Center, 975 N Warson Road, St. Louis, MO 63132 USA

Ivan Radin, Department of Plant and Microbial Biology, University of Minnesota, 1445 Gortner Avenue, Saint Paul, MN 55108 USA

Suruchi Roychoudhry, Centre for Plant Sciences, School of Biology, University of Leeds, Leeds, LS2 9JT. United Kingdom

Heather E. McFarlane, Department of Cell & Systems Biology, University of Toronto, 25 Willcocks St, Toronto, ON M5S 3B2, Canada

Corresponding Authors: Kirk J Czymmek (kczymmek@danforthcenter.org), Heather E. McFarlane (h.mcfarlane@utoronto.ca)

Short Title: Best Practices in Plant Cell Imaging

Materials Distribution Footnote: The author(s) responsible for distribution of materials integral to the findings presented in this article in accordance with the policy described in the Instructions for Authors (www.plantcell.org) is (are): Kirk J Czymmek (kczymmek@danforthcenter.org).

Abstract

Microscopy is a fundamental approach for plant cell and developmental biology as well as an essential tool for mechanistic studies in plant research. However, setting up a new microscopy-based experiment can be challenging, especially for beginner users, when implementing new imaging workflows or when working in an imaging facility where staff may not have extensive experience with plant samples. The basic principles of optics, chemistry, imaging and data handling are shared amongst all cell types. However, unique challenges are faced when imaging plant specimens due to their waxy cuticles, strong/broad spectrum autofluorescence, recalcitrant cell walls and air spaces that impede fixation or live imaging, impacting sample preparation and image quality. As expert plant microscopists, we share our collective experience on best practices to improve the quality of published microscopy results and promote transparency, reproducibility and data reuse for meta-analyses. We offer plant-specific advice and examples for microscope users at all stages of fluorescence microscopy workflows, from experimental design through sample preparation, image acquisition, processing, and analyses, to image display and methods reporting in manuscripts. We also present standards for methods reporting that will be valuable to all users and offer tools to improve reproducibility and data sharing.

Introduction

Imaging experiments can provide invaluable mechanistic and quantifiable insights into biological processes, and they have become essential for modern plant biology studies. Light microscopy is arguably the most widely used imaging approach in plants (Berg and Beachy 2008; Colin et al. 2022; Gilroy 1997; Ovečka et al. 2018). While other imaging approaches such as electron microscopy (Engel et al. 2015; Otegui and Pennington 2019; Wickramanayake and Czymmek 2023; Wightman 2022; Wilson and Bacic 2012), X-ray microscopy (Duncan et al. 2022; Piovesan et al. 2021), atomic force microscopy (Kirby et al. 1996), mass spectrometry imaging (Zou, Tang, and Li 2024), and high-throughput phenotyping (Fahlgren, Gehan, and Baxter 2015) have been applied for plant research, light microscopy dominates the literature in plant biology as an accessible, convenient, efficient and powerful approach to address important scientific questions in plant research. Fluorescence microscopy, in particular, can be used to localize fluorescently tagged proteins of interest in cells or tissues. The localization of cellular components, such as nucleic acids (Tirichine et al. 2009), polysaccharides (Piccinini, Nirina Ramamonjy, and Ursache 2024), lipids (Chu et al. 2022), hormones (Balcerowicz, Shetty, and Jones 2021; Herud-Sikimić et al. 2021), ions or other metabolites (Monshausen, Messerli, and Gilroy 2008) within cells or tissues are readily possible. In addition, fluorescent probes can be used to track developmental processes and cellular growth, compare wild type versus mutant or genetically engineered plants and/or compare control versus plants treated with external agents. Samples can be viewed live or fixed during microscopy experiments, depending on the biological question at hand. Often, components of interest (organelles, proteins, metabolites, etc.) will be tagged with fluorescent molecules such as fluorescent protein fusions in live or fixed cells (Berg and Beachy 2008; Haseloff 1999; Wu et al. 2013) including the convenient use of transient expression in tobacco leaves or protoplasts, localized via immunolabeling of fixed cells (Baskin et al. 1992; Lee and Knox 2014; Shimamura 2015), or identified using fluorescent stains (Hepler and Gunning 1998; Shaw and Ehrhardt 2013; Yu et al. 2008), all of which are widely used in plant biology. More sophisticated imaging approaches, such as Fluorescence Recovery after Photobleaching (FRAP) (Scheuring et al. 2024), Förster

Resonance Energy Transfer (FRET) (Krebs et al. 2012), Fluorescence Correlation Spectroscopy (FCS) (Clark et al. 2016), Fluorescence Lifetime Imaging Microscopy (FLIM) (Noble et al. 2017), Bimolecular Fluorescence Complementation (BiFC) (Waadt and Kudla 2008), multiphoton microscopy (Kurihara et al. 2015; Mizuta 2021), variable angle Total Internal Reflection Fluorescence Microscopy (TIRFM) (Wan et al. 2011) and expansion microscopy (ExM) (Cox et al. 2025; Kao and Nodine 2021) can be used to understand molecular interactions and their dynamics, but these techniques are outside the scope of this review, which is intended as a primer for novice and intermediate fluorescence microscope users.

Imaging experiments and analyses must be rigorously designed, and results must be judiciously interpreted and carefully communicated to ensure that the underlying data generated support the authors' claims. Indeed, there are numerous considerations and pitfalls that must be accounted for to achieve reliable, reproducible and meaningful results when using fluorescence imaging. Best practices in fluorescence imaging have been emphasized in several excellent overviews elsewhere (Lichtman and Conchello 2005; Montero Llopis et al. 2021; North 2006), and while many of the same guiding principles apply to plants, these use cases are typically focused on biomedical imaging using cell culture or animal tissue examples. Here, we provide practical guidelines focused on the fundamentals of fluorescence imaging and solutions for specific and unique challenges that plant biologists often face. These guidelines are aimed at beginning or intermediate microscopists but also offer standards that even advanced users could find useful. Like any scientific pursuit, excellence in imaging is an iterative process that is always grounded in the biological question being asked. We walk users through the steps of fluorescence imaging experiments from initial experimental setup, experimental design, sample preparation, image acquisition, through to data processing and analysis, image display and finally, methods reporting in manuscripts using plant-specific examples (**Fig. 1**). Importantly, before undertaking a large-scale imaging experiment we suggest a smaller pilot project with an expert mentor following the proposed imaging workflow (**Fig. 1**). Establishing a "design, test, learn, and iterate" mindset, creates a rapid feedback loop to address any unanticipated challenges and make to any refinements, accordingly. Our collective experience as instructors and microscopists has led us to emphasize the

common insights, misconceptions and pitfalls that newer users may experience. Ultimately, the goal of this manuscript is to help shorten the learning curve, improve experimental quality, foster reproducibility, and support success when fluorescence microscopy is applied to plant research.

1. Instrument & Fluorescence Probe Selection

Two of the most important upfront decisions when starting a plant imaging experiment are what probes to use and what type of microscope is best suited to answer the biological question. These two decisions are intrinsically linked. Ideally, one must consider the strengths and weaknesses of a particular imaging platform including assessment of the experimental requirements for lateral (x-y) and axial (z) resolution, acquisition speed, sensitivity (high signal collection efficiency), and spectral (wavelength) separation, in a concept referred to as “Dimensions of Imaging” **(Fig. 2**). While this chart represents common imaging modalities and their representative strengths/limitations, a majority of biological questions can be answered on any of these platforms, albeit with some technology-related constraints (reviewed by (Davidson 2024; Ovečka et al. 2018)). Practically speaking, many conventional widefield epi-fluorescence and/or confocal microscopes are suitable for many routine experiments.

1.1 Choosing an Imaging Platform

Widefield microscopes, which simultaneously illuminate the whole sample with a light source and collect emitted light, are likely to be the most accessible, flexible, affordable and easy-to-use option for plant scientists (**Fig. 3**). Although widefield epi-fluorescence microscopy is generally only suitable for thinner samples, deconvolution algorithms can partially restore resolution, contrast and signal using corrections derived from expected (theoretical) or measured (empirical) microscope performance (McNally et al. 1999; Swedlow 2007; Wernersson et al. 2024). The convenience and benefit of widefield microscopes should not be underestimated for many projects, especially for efficiently screening and documenting large sample sets , detecting weak signals (with high-end systems), and/or working with thin or thinly-sectioned materials. For example,

the out-of-focus blur observed using widefield microscopy of a thick plant leaf (**Fig. 3A**) can be partially resolved using deconvolution .

Laser scanning confocal microscopy (LSCM; also called point scanning confocal microscopy) is another primary workhorse for plant imaging experiments. LSCM excites fluorescent molecules using a laser focused to a point that is raster-scanned across the sample, and a pinhole aperture is used to reject out-of-focus emission light creating thin, high contrast “optical sections” (**Fig. 3B & C**). When 2D optical sectioning is combined with motorized focus control, z-stacks can be generated and reconstructed into 3D perspectives (**Fig. 3:** compare Widefield 3D, Confocal 3D & Super-Resolution 3D). A drawback of LSCM is speed (**Fig. 2**), since it takes time to raster the laser point-by-point across the sample. However, technology such as detector element arrays (e.g., Zeiss Airyscan) can further improve scan speed and resolution of LSCM (**Fig. 3G**) (Kana, Sediva, and Prasil 2023; Scipioni et al. 2018).

When higher imaging speeds are required for cell dynamics studies (e.g., calcium imaging, cytoskeleton dynamics, vesicle trafficking, or fast 3D collection (Oreopoulos, Berman, and Browne 2014; Ueda et al. 2010; Verbančič, Huang, and McFarlane 2021) spinning disk confocal microscopy (**Fig. 3E & F**) with multiple pinhole optics is often the tool of choice. Spinning disk confocal microscopy can capture data at imaging rates of ~100+ frames/second. Practically speaking, imaging rates will be much slower for many experiments. Fast imaging on spinning disk systems reduce photobleaching, relative to LSCM systems. Like LSCM, spinning disc systems can effectively be combined with the benefits of deconvolution (compare **Fig. 3E & F**).

Super-resolution microscopy (Hickey et al. 2021; Sydor et al. 2015) is appropriate when resolution is paramount to visualize features 2-10X below the diffraction limit (~250 nanometers with green light) such as with sub-organellar studies (e.g., localization of nuclear structures and pores (Schubert 2017), plasmodesmata (Bell et al. 2013; Czymmek, Duncan, and Berg 2023) and others as reviewed in (Komis et al. 2015; Ovečka et al. 2022)). A few common super-resolution techniques include single molecule localization microscopy (SMLM) approaches, such as photoactivated localization microscopy (PALM) and stochastic optical reconstruction microscopy (STORM), structured illumination microscopy (SIM) and Stimulated Emission Depletion (STED)

microscopy. With these more advanced techniques (Leung and Chou 2011), we strongly encourage consultation with an expert to assess feasibility and benefits/limitations for individual research goals.

Another factor to consider is whether the best microscope to use is upright (the objective lens above the sample) or inverted (the objective lens below the sample) or vertical (the objective lens and sample both horizontal). In general, upright and inverted configurations are readily amenable to traditional slide mounted specimens, although dipping lenses (that can directly contact the specimen medium) are primarily used with upright configurations (see *2.1 Tips for Working with Live Samples)*. Inverted microscopes can work well with certain live experiments where extra space or access above the objective lens is required, such as for a heating stage, manipulators or multi-well plates .

System performance is a function of the entire system's light path, including characteristics of all optical elements (filters, mirrors, objective lens, etc.) and the detector (a camera array versus point detector photo-multiplier tube (PMT)). For example, considering just the detector, high sensitivity scientific Complementary Metal–Oxide–Semiconductor (sCMOS) cameras can detect up to 95% of photons that reach it (referred to as its quantum efficiency (QE)) compared to ~45% for Gallium arsenide phosphide (GaAsP) photocathode (GaAsP-PMT) or 20% for traditional PMTs and these differences in sensitivities are also wavelength dependent (Montero Llopis et al. 2021). Ultimately, if weaker signals are anticipated, a more sensitive configuration may be critical.

1.2 Selecting Fluorescent Probes

Once the imaging approach is selected, it is important to determine what light sources/wavelengths and filters are available and to match these with the appropriate fluorescent probe. Here, widefield epi-fluorescence microscopy typically has some flexibility by using low cost and broad-spectrum white light (e.g., mercury or xenon arc lamps, metal halide lamps) or light emitting diodes (LEDs) as light sources (Aswani, Jinadasa, and Brown 2012). Most epi-fluorescence systems use filter cubes (containing filters and a dichroic mirror (specialized optical elements that differentially reflect/transmit light) to separate the excitation/emission light path (**Supplementary Fig. 1**) matched to the corresponding wavelengths appropriate for imaging the selected fluorescence

probe(s). While the majority of systems will have common filtersets for Blue (e.g., UV dyes, DAPI, Calcofluor White), Green (e.g., GFP, FITC, AlexaFluor 488) and Red (e.g., RFP, mCherry, Rhodamine, Texas Red, AlexaFluor 546, Propidium Iodide) fluorophores, other fluorophores (e.g., CFP, YFP) or longer wavelength fluorophores (e.g., chlorophyll A/B autofluorescence, Cy5 and AlexaFluor 660, or near-infrared probes) may require additional appropriate filters. Furthermore, filtersets can be long pass (having a wide emission range, e.g., 500 nm and all wavelengths above) or band pass (having a narrow emission range, e.g., 500 nm - 550 nm), and this distinction can have important implications for the experiment. For example, when working with leaf tissue, chlorophyll autofluorescence (650nm - 700nm) will often contribute undesirable signal (bleed-through or crosstalk) to the emission spectra of most lower wavelength fluorophores in the absence of band pass filters. Likewise, multiple fluorophore imaging almost always requires band pass filters to separate different fluorophores.

Many laser-based imaging systems, such as LSCM or spinning disk microscopes have discrete high-powered laser lines (e.g., 405 nm, 488 nm, 514 nm, 561 nm and 640 nm) or broader spectrum and/or tunable excitation ranges (e.g., white light or multi-photon lasers). Dichroic mirrors, filters, prisms, and/or diffraction gratings separate the excitation and emission pathways (**Fig. 4**) in laser-based systems. Notably, prisms and diffraction gratings in the emission pathway can be combined with sliders that are user definable, which allows flexible wavelength ranges and spectral imaging of fluorophore emission signals. Spectral imaging, in which a series of images collected at continuous discrete wavelength bands (e.g. 10 nm windows) along a defined spectrum (e.g., 400-600 nm) can be used to generate emission fingerprints and processed via linear unmixing to separate closely overlapping fluorophores. This capability is especially useful to help remove (unmix) various forms of plant autofluorescence that may contaminate target signals and/or to separate closely overlapping fluorophores (Conéjéro et al. 2014; Hardham 2012) to allow more fluorescent probes to be used in an experiment (Zimmermann et al. 2014). See **3.2 Controls** on strategies to ensure that crosstalk does not impact multi-color experiments.

Ultimately, the microscope's excitation and emission configuration and the fluorescent probes need to be carefully matched. However, there is some forgiveness

with filtersets and fluorophore choice, allowing sufficient excitation and emission signals to be collected even if not perfectly matched (e.g., a GFP filterset can be used to image YFP in many cases). Nevertheless, when fluorophore choice is flexible in experimental design and/or target molecule(s) are of low abundance and optimized conditions are critical, it is prudent to determine system light sources and excitation/emission configuration and to refer to excellent publicly available tools for optimizing probe choices with system configuration (**Fig. 4**). See FPbase.org (Lambert 2019) for fluorescent proteins, (SpectraViewer 2024) for common organic dyes, and (Colin et al. 2022; Malabadi, Teixeira Da Silva, and Nataraja 2008; Stewart 2001) for plant-specific genetically encoded probes.

When constructing genetically encoded fluorescent protein fusions, there are important considerations beyond fluorophore selection, including promoter selection and fluorescent protein fusion orientation. For example, the choice of promoter, fluorescent protein, and fusion orientation can all have profound effects on the behavior of actin binding fluorescent probes for visualizing the plant cytoskeleton (Dyachok et al. 2014; Wang, Yoo, and Blancaflor 2008). Additionally, consider using a monomeric version when working with fluorescent protein fusions i. Multimerization of fluorescent proteins is very common and while it can improve brightness, it can cause aggregation, affecting the localization pattern and/or function of target proteins (Campbell et al. 2002; Segami et al. 2014).

Ideally new fluorescent protein fusions are tested for functionality by the ability of the fusion protein to complement knockout mutant phenotypes before conducting imaging experiments.

Simply matching a fluorophore and system configuration is not always sufficient. The properties of a fluorophore also can play a role in imaging success, such as its pH/environmental sensitivity, size, photostability (resistance to bleaching) (Colin et al. 2022; Duwé and Dedecker 2019; Shaner et al. 2013; Tanz et al. 2013; Voss, Larrieu, and Wells 2013) and its overall brightness. Brighter probes allow for more gentle imaging (lower excitation power), improved signal-to-noise and faster acquisition times, which are all particularly important for live-cell imaging. The relative brightness of a probe can be calculated as the extinction coefficient (EC - likelihood of a fluorophore

absorbing excitation light) multiplied by the quantum yield (QY - the fraction of absorbed photons that result in fluorescence emission) divided by 1000 (McNamara 2024). For example, Enhanced GFP (EGFP) (EC = 55,900, QY = 0.6) has a relative brightness of 33.54 while mNeonGreen (EC = 116,000, QY = 0.8) has a relative brightness of 92.8 and is nearly 3X brighter. Although not all fluorophores are equal, many probes can be used interchangeably without issues. When flexibility is possible (e.g., starting experimental design from scratch) and/or the biological question demands specific conditions (low expression levels, high-speed imaging of dynamic events, multi-fluorophore imaging, autofluorescence challenges, etc.), optimizing probe choice for the biological question and the imaging system will increase the chances of a successful outcome and allow far greater versatility in imaging approaches across the dimensions of fluorescence imaging (**Fig. 2**).

2. Sample Preparation and Mounting

A critical step of successful plant imaging is sample preparation. There are at least four very important questions that should be part of that decision-making process: 1) Will the sample be live or fixed? 2) What microscope/objective lens is required to achieve the imaging goals? 3) How will the sample be mounted to ensure adequate optical quality? and 4) What controls are required to ensure that image features are not a result of optical, fixation, or other preparation-induced artifacts?

2.1 Tips for Working with Live Samples

Imaging living samples is usually convenient and fast (preparation steps are generally less involved) and since samples are not fixed, fixation artifacts can be avoided and dynamic events can be recorded. However, living samples are typically removed from their experimental growth conditions/environment and/or excised before mounting, which can cause substantial changes to the sample, including wounding responses and cell death. Indeed, some dyes tend to stain tissue more quickly at or adjacent to damaged or cut regions, leading to the temptation to image these sites (Truernit and Haseloff 2008). Users should avoid imaging areas of cell damage or death (unless scoring viability), since

these images will not be biologically relevant and will not reflect the reality of healthy, living cells (see 3.4 below).When working with aerial tissues, such as leaves, stems, or flowers, bubbles of air may be trapped between the epidermis and coverslip due to the hydrophobic waxy cuticle. These are relatively straightforward to identify as transmitted light images readily reveal the air bubble edge and the sample itself tends to have higher contrast in those areas. Avoid imaging within these regions as light scattering will severely impact optical quality and affect qualitative and quantitative results. Surface air bubbles can be reduced by adding surfactants such as 0.01% Silwet or Tween-20 (Huynh et al. 2022; Zhao et al. 2017) in aqueous sample mounting media. Intracellular air spaces can be infiltrated using gentle vacuum/syringe pressure to replace the air spaces in the spongy mesophyll with an aqueous medium to improve dye staining and optical continuity (**Supplementary Fig. 2**). When working with tissues that lack a waxy cuticle, particular care must be taken during sample preparation and mounting to avoid drying the tissue (Ovečka et al. 2018; Prunet, Jack, and Meyerowitz 2016; Sawchuk et al. 2007; Silveira et al. 2022; Zhu et al. 2020). For deep or long-term imaging, non-toxic and non-cell permeable media with low surface tension and excellent optical and gas-exchange properties may be useful, such as Perfluorodecalin (a component of artificial blood) and its derivatives (Littlejohn et al. 2010, 2014). Long-term imaging under the coverslip may lead to the compression of observed samples, which can influence the organization of structures such as the microtubule cytoskeleton, which is mechanoresponsive (Hamant et al. 2008; Jacques, Verbelen, and Vissenberg 2013). These effects can be partially mitigated by using adequate spacers between mounting slides and coverslips that prevent mechanical compression of the tissue and by reducing water evaporation during imaging. For many developmental studies, a more specialized lightsheet (Ovečka et al. 2018) or upright microscope configuration with dipping lenses are often the best choice, if available (Silveira et al. 2022; Zhu et al. 2020). When using dipping lenses, samples are often mounted on agar medium in small Petri dishes or other plastic containers. The presence of air bubbles on the surface of the sample and sample movement can pose problems when imaging with dipping objectives, requiring additional preventive measures to avoid artifacts such as localized signal loss and geometric distortions of the sample (Prunet et al. 2016; Sawchuk et al. 2007).

352

353 *2.2 Tips for Working with Fixed Samples*

354 For fixed samples, a broad range of affinity probes are available, such as stains,
355 antibodies, or *in situ* hybridization to detect nucleic acids. Additionally, with appropriate
356 fixation protocols, fluorescent protein signals can be retained (Kurihara et al. 2015; Nybo
357 2012). Samples can be fixed, typically in aldehydes, and imaged intact as a whole mount
358 (Kurihara et al. 2015; Truernit et al. 2008) or prepared for sectioning via hand sections,
359 vibratome (Leroux 2020), cryostat (Knapp et al. 2012; Tirichine et al. 2009) or microtomy
360 (Baskin et al. 1992; Marion et al. 2017). Which sectioning approach is most appropriate
361 will depend on tissue type and size, desired section thickness, probe accessibility needs,
362 and the capabilities of the selected imaging platform. Generally, hand sections will be
363 thicker (millimeter scale) and more variable, vibratome and cryostats can reliably produce
364 sections (tens of microns), while microtomy of resin embedded specimen can yield
365 sections ranging from tens of nanometers to a few microns. To identify an appropriate
366 sectioning strategy, we suggest identifying a publication with similar probe types and
367 imaging goals and/or contacting a domain expert. Antibodies and other larger probes can
368 be used to label sections, or with special treatment to disrupt or remove plant cell walls,
369 such as enzyme or chemical permeabilization, or freeze shattering methods (Celler et al.
370 2016; Shimamura 2015) these large probes can be applied to whole-mount samples.
371 Notably, the fixation strategy and buffers themselves can induce artifacts (Yoshida, Maity,
372 and Chong 2023). When working with fixed specimen, autofluorescence can be a by-
373 product of aldehyde fixation, especially glutaraldehyde. Use of 0.1% sodium borohydride
374 (Clancy and Cauller 1998) can help reduce aldehyde induced autofluorescence, and
375 addition of glycine to block unreacted aldehydes (Piña et al. 2022). In some instances,
376 samples can be cleared (Hériché et al. 2022; Kurihara et al. 2015; Sakamoto et al. 2022)
377 and/or mounting media with/without antifade components can be applied to improve the
378 optical homogeneity throughout the sample for high quality, deeper imaging (Bassel and
379 Smith 2016). Photobleaching results in chemical modification of a fluorophore
380 (Mahmoudian et al. 2011) causing the irreversible loss of fluorescence. Antifade agents
381 are chemical compounds that serve as oxygen free radical scavengers, which can reduce
382 photobleaching. However, not all anti-fade agents are created equal, and many do not

work effectively or universally for all probes and are toxic for living cells (Ono et al. 2001). For further reading to help select an appropriate mounting media, we recommend an excellent primer describing various mounting media components and comparing their performance (Collins 2006).

2.3 The Objective Lens, Immersion Medium, Coverslip, & Mounting Medium

For high-resolution imaging of live or fixed samples, the sample mounting medium (the media in which the sample is suspended in between the slide and the coverslip) should be considered as an extension of the objective lens. The mounting medium should be an optically- and sample-suitable solution (water, buffer, etc.) that considers both the sample and the objective lens.

Many objective lenses are labeled to use a specific immersion media (the media between the objective and the slide coverslip; e.g., air, water, oil) to achieve their designed performance specifications. With the exception of air lenses, a small droplet of immersion media is placed between the front lens element of the objective and the sample coverslip , ensuring optical continuity (no coverslip is used with a dipping lens - see *2.1 Tips for Working with Live Samples*). For more detailed background reading, we highly recommend an excellent overview of the important characteristics and concepts of immersion media (Abramowitz and Davidson 2015).

Importantly, the NA of an objective lens has a dependency on the refractive index (RI) of the immersion medium (Keller 1990; Staudt and Hell 2008) and the more closely matched and uniform the RI of the objective immersion medium is to the sample and its mounting medium, the better the image quality (compare **Fig. 5A and B**, air vs water infiltration). In simple terms, the objective lens numerical aperture (NA) essentially relates to the cone of light that is collected by the lens and represents its light gathering and x-y-z resolving power. For reference, common objective immersion media are as follows; air (RI = 1), water (RI = 1.33), glycerol (RI = 1.47), silicone (RI = 1.4) or oil (RI = 1.51). For example, this is illustrated by imaging a uniform 3% agarose gel (RI ~1.33, like many biological tissues) infiltrated with 1µg/ml of fluorescein isothiocyanate (FITC) demonstrating the effect of the objective lens on signal intensity from the coverslip to ~300 um deep (Supplementary Fig.3). In this homogeneous sample, there is a notable

decrease in signal when using the 20X air lens (NA 0.7) and excellent uniformity with the 40X water lens (NA 1.2). Although there is substantial signal attenuation with the highest NA 100X lens (NA 1.4), the 100X lens outperforms these other lenses in resolution when imaging very near the coverslip (**Supplementary Fig. 4**). This example demonstrates the tradeoff between high resolution imaging with a low depth of imaging (e.g. with the high NA, 100X oil objective) and low-resolution imaging with a greater depth of imaging (e.g. with lower NA, 40x water objective). Additionally, even in this relatively uniform sample (**Supplementary Fig. 3**) and in more complex plant samples (**Fig. 5**), image quality and resolution are degraded due to spherical aberrations (Diel, Lichtman, and Richardson 2020; Goodwin 2007) that increase in severity at increasing distances from the coverslip due to RI mismatch. This means the image quality, resolution and signal intensity can degrade rapidly away from the coverslip, compounded by many light-scattering plant structures. Even slide-to-slide variations in mounting medium thickness covering the sample can make a measurable difference in fluorescence signals and image quality. Nevertheless, in some instances, it is worthwhile to verify specific experimental requirements and compare images acquired with different objective lenses, for example, a higher NA 100X lens versus a 40X oil objective (**Supplementary Fig. 4)**.

Using the proper coverslip is another important component of the optical path, since it will be placed between the sample and the objective lens. The coverslip is therefore included as part of lens design and impacts how light is focused on and collected from the sample. Deviations in coverslip thickness from the manufacturer's specification (typically No 1.5 for high NA lenses) can have a pronounced impact on image quality and data quantification, causing decreased resolution and contrast (Fellers, Thomas J.; Davidson 2024). Even when using the proper coverslip, care must be taken that it is perpendicular to the objective, as tilted coverslips covering thick or uneven samples increase the apparent thickness of the coverslip and introduce asymmetrical aberrations and signal degradation.

3. Experimental Design, Image Acquisition and Instrument Settings

3.1 Experimental Bias

When designing any experiment, steps should be taken to minimize bias. Experimental biases can affect experimental outcomes and compromise reproducibility, potentially leading to skewed data acquisition, analyses, and conclusions (Lee et al. 2024; Munafò et al. 2017). Biases during image acquisition emerge from two main sources: 1) sample bias, i.e., when specific sections, regions, technical and/or biological replicates are selected for imaging and 2) human/unconscious bias, i.e., visual perception is biased toward the detection of certain features in a non-quantitative way, and thus cannot provide reliable information (Brown 2017; Jonkman 2020; Jost and Waters 2019). Bias can be managed with good experimental design, which may include technical and biological replicates, use of appropriate controls, blinded/randomized samples, automated acquisition, and increased sample size using tiling and/or z-stack acquisition modes. Before acquisition, it is important to set up ways to track raw data, acquisition settings, image processing steps and other parameters that will be required for analysis (Lee and Kitaoka 2018). Steps to limit biases, sample size, number of replicates and any sample processing before imaging should be reported accurately when preparing images for publication.

3.2 Controls

Controls are required for the proper interpretation of any scientific data (Baker 1984; Lipsitch, Tchetgen Tchetgen, and Cohen 2010; Torday and Baluška 2019), and microscopy is no exception. While controls will be specific for each experiment, common themes emerge. As in any biological experiment, biotic, abiotic and/or chemical treatments need to be compared to mock treatment (i.e., vehicle only) and mutants need to be compared to wild-type control samples. However, imaging experiments also require additional controls. For example, the expression level of genetically encoded reporters (e.g., GFP-fusion proteins) can have a profound effect on their observed subcellular localizations (Lisenbee, Karnik, and Trelease 2003). Fusion proteins should be tested for functionality by their ability to complement corresponding mutant phenotypes and it is best practice to confirm the molecular weight of the fluorescent protein-fusion protein via western blotting to ensure that the fluorophore is not cleaved from the protein of interest (Moore and Murphy 2009). When using affinity probes such as antibodies for

immunolocalization (Baskin et al. 1992; Guerin 2023a, 2023b; Shimamura 2015), important negative controls include the use of non-immune serum, pre-immune serum (when available) and samples treated without a primary antibody, but otherwise underwent all of the same processing steps as immunolabelled samples. For nucleic acid localization via *in situ* hybridization, a scrambled probe is an essential negative control (Jiang 2019; Prieto, Moore, and Shaw 2007). Staining protocols should always compare stained samples to unstained controls to evaluate background signal and autofluorescence. Establishing an imaging pipeline with appropriate positive and negative controls is essential to obtain reliable, meaningful and reproducible data, both to enhance interpretation and assist in troubleshooting experimental anomalies.

3.3 Autofluorescence and Imaging Multiple Fluorophores

Experimental conditions should also be established considering background autofluorescence and bleed- through. Plants produce many autofluorescent compounds - both generalized and environmentally induced and species/tissue specific. Autofluorescent compounds are often found in the cell wall, plastids or vacuole but may also be cytosolic. Common autofluorescent compounds in plant samples include cell wall lignin in the blue range (400-440 nm), chlorophyll in the red/far-red range (600-800 nm), and cell wall (grasses) or phloem (conifer) ferulic acid/ferulate in the blue range. (Donaldson 2020). Stressed or dying cells often produce secondary metabolites that autofluoresce in the cytosol or vacuole. We refer readers to a detailed list and associated spectra (Donaldson 2020). Autofluorescence will often appear in multiple channels, so checking for fluorescent signals across multiple channels will help identify if a signal is "real" and also identify the best wavelength range for the probe. To further discriminate between autofluorescence and "true" signals, appropriate controls should be used. For example, non-transgenic plants, when using genetically encoded fluorescent reporters (e.g., GFP) or unstained plants, when using dyes or immunofluorescence, should be imaged using identical acquisition settings. The mere presence of autofluorescence does not in itself prevent useful imaging results if proper controls are used; for example, strong fluorescence from the selected probe(s) can often overcome weak or tissue/organelle specific autofluorescence. (Clancy and Cauller 1998)(Piña et al. 2022). If the

autofluorescence emission is at a wavelength that is not collected for other fluorophores in the experiment but provides useful cell structure markers (e.g., cell walls , vacuoles, chlorophyll etc.) it can provide useful context in imaging studies.

When using multiple fluorophores, an important control is to check for and apply strategies to minimize/eliminate bleed-through into other channels (**Fig. 4**) which can also result in misassignment of emission signals, and particularly false “co-localization”. For example, many commonly used dyes, such as propidium iodide and FM4-64, have broad excitation and emission spectra that can be detected across multiple channels. Therefore, a useful approach is to image a specimen across multiple channels to determine if there is any channel bleed-through and then apply strategic selection of excitation wavelengths, sequential imaging and emission filters to limit any crosstalk. (**Fig. 4C-F**). The sequential excitation and emission strategy (one fluorophore being exited and imaged at a time) along with judicious emission filter settings, is very effective to reduce/eliminate crosstalk of compatible multi-color fluorophore combinations (**Fig. 4C-F**); however, sequential imaging will be slower compared to a simultaneous approach.

When planning to conduct fluorescent intensity measurements, best practice is to image a second fluorophore that should not change under experimental conditions. For example, nuclear-localized fluorescent proteins have been used as internal standards to conduct ratiometric measurements of fluorescent intensity of secreted GFP (Samalova, Fricker, and Moore 2006) and during bimolecular fluorescence complementation (BiFC) experiments (Grefen and Blatt 2012). Autofluorescence can also be useful in this context.

3.4 Controls for Live-Cell Imaging

Live cell imaging experiments need to be carefully monitored to avoid imaging dying or dead cells. Best practice includes imaging samples for the shortest possible time; however, with careful sample preparation and appropriate controls, images can be collected over days or even weeks (Czymmek et al. 2004, 2007; Le Gloanec et al. 2024; Gómez-Felipe et al. 2024; Hervieux et al. 2016; Schneider et al. 2022). Environmental conditions should be monitored and controlled, including sample temperature and light conditions, since these can affect cellular dynamics and organization (Fujita et al. 2013; Lindeboom et al. 2013; Wang et al. 2020). Tissue dehydration can also adversely affect

imaging, especially for tissues without a waxy cuticle, such as roots. Although the signs of decreasing cell health can vary, some indicators of “dead cell imaging” include decreased or cessation of cytoplasmic streaming and Brownian motion (wiggling) of subcellular components (Chow, Mohammad, and McFarlane 2025); fragmentation of the plasma membrane, vacuole, ER network, and cytoskeletal networks; increased autofluorescence; or cessation of cellular growth. Vital stains can be used to determine whether cells remain alive during established imaging conditions; for example, although propidium iodide is a common counterstain for plant cell wall outlines, and it will stain the cytoplasm and nuclei when the plasma membrane (cell viability) has been compromised (Hoffmann, Mohammad, and McFarlane 2024). Fluorescein diacetate (FDA) or SYTOX™ dyes (Truernit et al. 2008) are other cell viability stains that can be effectively used in plants (Jones et al. 2016). Finally, when imaging cells and/or organs, especially for long imaging experiments, it is prudent to ensure imaging experiments do not alter sample biology. Best practice is to monitor a control specimen that is not subjected to the microscopy experiments to determine if there are differences in the size, shape and developmental stage compared to the imaged specimen.

3.5 Instrument Settings

Acquisition settings must be consistent when performing quantitative image comparisons. For example, if fluorescence intensity is being compared, the same microscope and acquisition settings (e.g., detector settings (offset/gain), pixel or frame exposure time, averaging, image size, filters, excitation power, objective lens) must be used to image control and test samples. Indeed, many commercial systems conveniently have a “reuse” (or equivalent) function to allow users to reload hardware/software settings from previously acquired data. Although convenient, not all settings may automatically be reapplied so the stored image metadata should be carefully compared with “reuse” settings for all imaging sessions.

There are dozens of instrument settings, many often not readily apparent, that can influence measurements for quantitative fluorescence microscopy such as system alignment or laser/light source stability (Pawley 2000). For system hardware, periodic system alignment, regular cleaning and other tests using standard slides by the

responsible core facility or system manager should be performed for quality control assessment of the imaging system. Recently, a kit for evaluating system performance has become available by loan from Bioimaging North America to assess and ensure reproducibility (BINA 2024; Gaudreault 2022; Nelson 2022).

3.6 Background and Dynamic Range

Background signals are common in many imaging experiments and will vary by detector type. For example, widefield and spinning disk microscopes have cameras (rather than point detectors like PMTs, or comparable, which are common on LSCMs) and it is common to have gray rather than black (pixels with a zero-intensity value) backgrounds. There may be a temptation to adjust contrast (gain) and brightness (offset) settings, especially on LSCMs, to reduce/exclude background or unwanted signals, increase contrast or to emphasize a feature of interest. Image acquisition conditions should be adjusted to avoid excessive under- or over-saturated pixels (blue or red, respectively in (**Fig. 6C-E**) to prevent "clipping" or truncation of the data, which can hinder reliable interpretation, cause loss of features and compromise the ability to quantitatively analyze the image. During acquisition, this can be done by adjusting exposure/pixel dwell time, exposure time and or camera/detector contrast and brightness (gain and offset) settings. These same settings should be used to image all samples in a given experiment (i.e., wild type and mutant, or control and treatment). When first setting-up experimental conditions, we recommend leveraging the "range indicator" option available on many imaging systems that will apply a single color to represent black (e.g., blue assigned to 0 intensity pixels in an 8-bit image) and saturated/white pixels (e.g., red assigned to 255 intensity pixels in an 8-bit image), while all pixel intensities in between these extremes remain greyscale (**Fig. 6C-E**). Alternatively, a histogram of the image can be generated, representing the pixel intensity distribution of the entire image (**Fig. 6C'-E'**), for experimental set-up or post processing to reveal "clipping". For quantitative settings across images, it is important that images reflect the truth in a comparable manner, rather than offering an artistic or aesthetically pleasing image. For fluorescence quantification, images should only be acquired using consistent settings without over- and under-saturated pixels, as these pixels can skew the results. An exception to this rule is the

acquisition of channels used to determine cell outlines for 2D/3D segmentation because many image analysis software packages can better detect cell outlines when the signal is strong (Wang et al. 2025).

3.7 Photobleaching

Even if settings are identical and the imaging system stable, other hardware dependent settings, such as the laser/light power at the sample can adversely impact results. Notably, photophysical effects such as photobleaching can cause an irreversible loss of fluorescence due to a chemical modification of the fluorophore in the presence of light and free radical oxygen (Mahmoudian et al. 2011). These issues are especially problematic when collecting z-stacks or time-lapse experiments (compare **Fig. 7A & B** with **Fig. 7C & D**). While improved fluorophore design and free radical scavengers (anti-fade agents; see also 2.2) help mitigate photobleaching, light/laser power and exposure/dwell time settings can also be adjusted to limit photobleaching depending on microscope platform. A quick check to assess photobleaching is to measure the intensity of the sample over time; non-linear intensity-changes over time indicate that significant photobleaching is occurring (**Fig. 7E**). Photobleaching can be reduced by lowering the laser power (in this example from 0.8% to 0.08%) and plotting intensity over time until average intensity remains constant over the expected imaging duration (**Fig. 7E**) and/or by decreasing image collection time, either by decreasing exposure time on camera-based systems, or by increasing scan speed in LSCM systems. Additionally, cropping an image (scanning a smaller bounding area), while maintaining the same pixel resolution with point scanning microscopes is an effective way to limit bleaching of larger tissue areas and increase scan rate. However, zooming to reduce scan area can potentially increase photobleaching and has a squared relationship to the zoom factor. For example, zooming from 1 to 2 concentrates the same amount of excitation light into one-fourth of the area, zooming from 1 to 3 into one-nineth, etc. While lower excitation light and/or faster image collection will decrease signal-to-noise (image quality), keep in mind that noise is inherently present in all images and when the goal is to capture and measure a dynamic process or large volume, maintaining the integrity of the data should outweigh simply having an aesthetically pleasing dataset.

631

632 *3.8 Objective versus Pixel Resolution*

633 The resolution of a given objective lens is fixed and determined by its NA and the
634 wavelength(s) of light being used, known as Rayleigh Resolution Limit (Pawley 2006).
635 The theoretical Rayleigh lateral resolution for an objective lens for fluorescence is
636 calculated: 0.61(**λ**)/NA, and for axial resolution (optical section thickness): 1.67(**λ**)/(NA)^2
637 (Jonkman et al. 2003, 2020), where **λ** = wavelength of the fluorophore . Thus, for a GFP
638 fluorophore (530 nm peak emission) and 40X 1.1 NA lens, the Rayleigh resolution is
639 calculated to be 294 nm, and optical section thickness of 731 nm. However, depending
640 on the number of final pixels in an image, often the full resolving power of the objective
641 lens is not captured, and may not always be needed. If the full-resolution of the objective
642 is required for an experiment, Nyquist sampling must be met, namely, there must be
643 sufficient spacing of pixels in a 2D and/or 3D image to oversample the smallest resolvable
644 structure by two to four-fold (Pawley 2006). For example, a selected 2D field-of-view
645 imaged with 2048x2048 pixels (pixel size 57 nm) meets the Nyquist sampling for the 40X
646 1.1 NA lens (**Fig. 6A**), while using 128x128 pixels (pixel size 918 nm) (**Fig. 6B**) falls far
647 below and subtle features may be lost in an under-sampled image. However, if the goal
648 is simply to count the number of cells or measure cell perimeters, the smaller image size
649 is perfectly adequate, has a smaller file size and is ~250 times faster to collect.
650 Undersampling also can be accomplished by increasing the scan speed by using a
651 smaller frame size on a LSCM system, or by "binning" an EM-CCD (i.e. grouping a square
652 of 2x2 adjacent pixels together into one larger pixel). Importantly, binning can also help
653 with detection of weak signals. It is worth keeping in mind that most journals require 300
654 dots per inch (dpi) pixel resolution for figures. Thus, a 512 x 512 pixel image will be ~1.7
655 x1.7 inches at 300 dpiresolution and this may be inadequate to display the desired feature
656 without acquiring at greater pixel resolutions or interpolation (Fig 6A & B).

657

658 **4. Image Processing & Analysis**

659

660 Image processing and analysis are expansive topics and advanced image
661 processing or analyses are beyond the scope of this primer. Processing and analysis can

occur in a variety of software programs, including software that is used for acquisition (such as Nikon Elements, Leica LAS-X, Olympus FluoView, or ZEISS Zen), open source software such as ImageJ, specifically the Fiji distribution (Schindelin et al. 2012), or specialized software such as Imaris, Huygens (Day et al. 2017), CellProfiler (Stirling et al. 2021) or MorphoGraphX (Barbier de Reuille et al. 2015; Strauss et al. 2022). Here, we focus on the basics that every plant microscopist needs to address. We will briefly discuss common fundamentals, but refer readers to several excellent general reviews that cover topics such as optimizing image acquisition settings, enhancing image quality, and performing basic measurements for data analysis (Bassel and Smith 2016; Hickey et al. 2021; Hobson et al. 2022; Russ 2006; Waters 2009).

4.1 Documenting Processing Steps

Image processing steps include anything that changes an image from its original form. These may include seemingly mundane changes such as adjustments to intensity (e.g., brightness/contrast), background subtraction or thresholding, smoothing or sharpening filters, applying lookup tables (false color of images), cropping, rotating, merging channels, changing bit-depth or resolution, creating z-projections or 3D reconstructions and image compression, to name a few. It can also include more advanced processing, deconvolution, segmentation, or use of artificial intelligence with machine- or deep-learning approaches. Importantly, all of these image processing adjustments can alter the pixel values of images, which can dramatically affect any subsequent quantitative image analyses (Halazonetis 2005; Russ 2006). Understanding how detectors (Spring 2001) and processing steps can impact quantitative data will help microscopists make good decisions about processing and analysis (Pawley 2006). For example, when exporting images to work with other software, many confocal microscopes acquire images with dynamic ranges of 8-bit (256 pixel gray levels), 12-bit (4,096 pixel gray levels), or 16-bits (65,536 pixel gray levels), while RGB color images are typically at least 24-bit (8-bits/channel, 16,777,216 colors). When given the choice, 16-bit images (or system maximum) are preferred, as images can be down-scaled to 8-bit for display purposes, but it can’t be reverted to 16-bit without loss of information. Likewise, when capturing and/or saving screenshots, color images are typically 8-bit RGB (only 256 total

colors) and screenshots do not match the raw data pixel intensity values. Thus, conversion from 16- to 8-bit necessarily rescales the image. Also note that all detectors (point or camera-based) are simply collecting photons which are converted into a digital signal where the relative number of photons collected represents the intensity of the sample at a given position. RGB cameras use a color filter array and point detectors, such as PMTs, leverage user defined emission filters for each fluorescent channel. In either instance a Look Up Table (LUT), black and white or color is typically assigned to reflect the intensity range (Spring 2001). Quantification of pixel intensities must always be done on the original, full bit-depth images, and when converting to 8-bit for display, users should be aware of the image scaling impact. For example, **Figure 6C & D** shows an example of a single image acquired at one setting but displayed at different intensity scales. Digitally rotating images usually involves interpolating pixel information, which will also change pixel values. Assembling figures in PowerPoint or other presentation software, while convenient for presentations, has the risk of intentional or inadvertent changes in aspect ratio and image data compression, depending on settings. Likewise, converting images to different types (e.g., from TIFF to JPEG) to save disk space or for portability with other software results in lossy image compression which will impact the quantitative and qualitative information in images (**Fig. 8**) and should only be used for presentations, websites or communications where file-size is limiting. An acceptable option, if space is a concern, is lossless compression formats of TIFF for multi-channel or z-stacks, or PNG files for single images. Overall, when comparing fluorescence intensity between samples, best practices include applying the same preparation steps to all samples, using the same acquisition settings to gather all data, and applying the same processing steps (avoiding irreversible file compression-based loss) to each image before data analysis.

Analysis routines can also range from simple to sophisticated and can be highly customized for specific applications. In general, image analyses involve extracting quantitative information from images, such as object size, object intensity, or the relationship between objects (e.g., ratiometric imaging (Ast et al. 2017; Samalova et al. 2006), colocalization (Lathe et al. 2024), or kymographs (Verbančič et al. 2021; Zhou et al. 2020). Since analyses rely on quantifying pixel/region intensity and/or coordinate values from images, and processing steps will change these values, it is best practice to

conduct analyses on minimally processed or unprocessed images. It is also essential for users to report the software used (including version number) for image analyses, and all details of any segmentation and analysis steps applied (including parameters/settings in any algorithms applied), and how regions of interest were selected for analysis.

4.2 Image Analysis in Biological Context

Plants have several unique features that should be specifically considered during image analyses. These include autofluorescence, rapid cytosolic streaming, and large central vacuoles. As discussed in 3.3, appropriate controls should be used to assess whether autofluorescence is contributing to the image and to minimize these contributions, especially for any quantitative analyses. For any live-cell imaging experiments, microscopists should consider whether rapid cytosolic streaming might be a confounding factor, since cellular contents can move at speeds up to 4.2 $\mu m\ s^{-1}$ (Nebenführ et al. 1999) which may be faster than the interval between images. In z-stacks, cytoplasmic streaming can alter the shape of objects, creating an elongated object (Nebenfuhr et al 1999;). In colocalization experiments, cytosolic streaming can decrease the degree of colocalization (Ebert et al. 2018) . The large central vacuoles in many plant cell types, including protoplasts and *N. benthamiana* leaf epidermal cells, will push cytoplasmic contents to the edge of the cell, which can cause cytoplasm, ER, tonoplast membrane or plasma membrane signals to be mistaken for each other (**Fig. 9**). Such mistakes can be avoided by colocalization of known markers with the construct of interest. Markers that positively identify many subcellular compartments with different fluorophores are available from stock centers (e.g., the Arabidopsis Biological Resource Center (ABRC) or Eurasian Arabidopsis Stock Centre (uNASC)) for a nominal fee as constructs for transient co-transformation (Nelson, Cai, and Nebenführ 2007) or as stable Arabidopsis lines for crossing (Geldner et al. 2009). Alternatively, FM4-64 and PI counterstaining can differentiate between the plasma membrane and the cell wall, respectively, with some exceptions depending on tissue type and image modalities (Galvan-Ampudia et al. 2020). In either case, generating a line scan by drawing a line perpendicular to the plasma membrane and plotting fluorescent intensity of the marker compared to the probe of interest over the length of the line will illustrate whether the

intensity peak of the signal of interest matches the intensity peak of the marker line or counterstain (**Fig. 9D-F, inserts**). Z-stacks can also help to differentiate between different compartments, since ER-localized proteins will show characteristic web-like architecture in the cortical cytoplasm and peri-nuclear signal (**Fig. 9A-C**).

4.3 Image Manipulation, Image Integrity and Use of Artificial Intelligence

As discussed (see 3.1), human bias can be a large contributing factor in collecting and interpreting data. For microscopists this is further compounded in the digital era by the relative ease with which images can be adjusted, converted or otherwise modified in numerous places along a workflow. Indeed, it was reported that ~2% of accepted papers have either inappropriate modifications and/or manipulation, which can result in misrepresentation of the data (Cromey 2010; Martin and Blatt 2013) or insufficient reporting details (Marqués, Pengo, and Sanders 2020) Often in our experience, improper data handling can be unintentional and/or caused by lack of training. Furthermore, considering the power, potential and rapid adoption of artificial intelligence (AI), a growing number of scientific hardware and software solutions (including generative AI) can automate finding, collecting, processing, segmenting, visualizing and analyzing data (Wang et al. 2023). However, the same rules for data analysis and reporting apply when using AI. Namely, any approach that modifies or processes data, AI or other, must be accounted for, users should understand the consequences of these analyses and all processing steps must be reported with sufficient detail to ensure reproducibility. Furthermore, since AI models and training data are evolving rapidly, simply using the same tool does not assure reproducible analyses, especially when using proprietary or otherwise opaque image processing algorithms, and results may vary unless the same version is used and/or a fixed model and training data are used for processing and all analyses.

4.4 Image Annotation and Presentation

The specifications of figure assembly are typically provided by each journal, but microscopists must make many decisions about how to display and communicate data. Researchers have created community-driven checklists to improve the quality and

reporting of microscopy images in publications (Schmied et al. 2024). These resources offer practical guidance on image preparation, including formatting, color choices, and data sharing, as well as best practices for describing image analysis workflows. Basic image annotations should always include scale bars, plus time stamps, if applicable. If multiple images are to be compiled and compared (e.g. wild type vs mutant) matched magnification and a common scale is best. Insets or additional panels, either showing a tissue overview or a zoomed-in view may help orient the reader or highlight elements of interest at increased detail. Similarly, if a z-projection is being performed and images are being compared, the same method (e.g., maximum intensity projection) must be used, and the number of planes projected should be reported and ideally the same amongst samples. When displaying a single channel and/or transmitted light, side-by-side grayscale images are best, as we have done herein (Figs. 6 & 9). When displaying multi-channel or multi-color images, application of a cyan, yellow, magenta, green and/or grayscale color-schemes are the most accessible to readers and avoid using a combination of colors that are indistinguishable for color blind people (Jambor et al. 2021); we have provided several different examples of suitable color combinations throughout this manuscript (**Figs. 3, 5 & 6**).

5. Reporting

5.1 FAIR Principles and Public Repositories

Comprehensive reporting is essential for accurate research communication, reproducibility, and data accessibility/reusability. Findability, Accessibility, Interoperability, and Reusability (FAIR) guiding principles outline best practices for data management (Wilkinson et al. 2016). Unfortunately, microscopy methods and micrograph analyses are often vaguely or incompletely described in publications (Heddleston et al. 2021; Marques et al. 2018; Montero Llopis et al. 2021). The responsibility to improve reporting lies with authors, reviewers, editors and ultimately with scientific journals. However, we recognize that the complexities of these considerations may be daunting for novice microsocpe users or non-expert reviewers. As a companion, and not replacement for written materials and methods, we provide a straightforward reporting spreadsheet

template (**Supplementary Table 1**) that can be used as a convenient approach to manage details about the samples and imaging setup for each figure. Excellent alternatives are also available to meet diverse lab needs (Heddleston et al. 2021). Ideally, all corresponding original raw data underlying images in the vendor's native format and methods are deposited in an open and public data repository, such as Zenodo (Sicilia, García-Barriocanal, and Sánchez-Alonso 2017) or Open Science Framework (OSF) (Foster and Deardorff 2017). Depending on file size and data type, other publicly funded repositories such as BioImage Archive (Hartley et al. 2022) or Electron Microscopy Public Image Archive (EMPIAR) (Iudin et al. 2016, 2023) may be appropriate. Sharing data via repositories also permits data reuse or meta-analyses by the community. An unambiguous organizational schema for image classification that includes sample type (plant, tissue, and cell type), fluorophore/stain, instrument and image acquisition parameters, and any processing steps can facilitate data reuse. While this framework for representing fluorescence imaging data does not currently exist in a mature form and data size is still an issue, other databases, such as the Protein Data Bank (Burley et al. 2019), may offer useful lessons for establishing community driven data frameworks, similar to the macromolecular Crystallographic Information Framework (mmCIF), the data standard for structural biology (Westbrook et al. 2022). For now, accurate recording and reporting of all imaging experiment steps promotes reproducibility and can support troubleshooting when experimental outcomes vary or are unexpected. Importantly, good reporting goes hand-in-hand with thoughtful experimental design and recording from the very beginning of the process, thus we recommend consulting the reporting spreadsheet template (**Supplementary Table 1**) (or a similar alternative) prior to starting each experiment and while conducting experiments.

5.2 Sample Treatment and Microscope Settings

As discussed above, many factors can dramatically influence microscopy data and these must all be reported. For example, the specific fluorophore used or manufacturer and catalog number of any antibodies or dyes must be reported since their spectral and binding properties can vary greatly. Likewise, for fixed samples, a detailed protocol will include manufacturer and catalog numbers for all reagents plus concentration and timing

for key steps, such as fixation, washes with buffers and incubation with antibodies. For live cell imaging, environmental conditions during the experiment can have a strong effect on plant cells and the biological phenomenon being studied, including ambient temperature and light conditions, and/or how live tissues were oriented relative to the gravity vector (von Wangenheim et al. 2017) (**Supplementary Fig. 5**), so these should also be reported. Similarly, microscope characteristics and settings such as imaging modalities, objective properties, excitation and emission optics, and image collection parameters must be reported (**Supplementary Table 1**).

5.3 Image Analysis and Statistics

Image analysis details must also be reported since software for image processing is constantly evolving. In general, the program/software must be reported (manufacturer and/or citation to publication, including version number), as well as any details of the algorithms applied to the images and the parameters/settings used for application of these algorithms. Some examples include details of brightness & contrast adjustments, background subtraction, denoising, deconvolution, thresholding, and segmentation (Aaron and Chew 2021). Sufficient detail for reproducibility should be provided for any quantification, such as which tissues and cell types were used for quantification, how features were selected for measurements, and how the sample size was calculated. P-values are often dramatically overestimated in microscopy experiments (also called “p-hacking”) by measuring multiple events/objects from a single biological organism or cell but counting each of these events/objects as independent biological replicates (Lord et al. 2020). For example, if 10 plastids were measured from one control plant and 10 plastids were measured from one inhibitor-treated plant, then n = 1 for each condition, since differences in the plastids could simply be due to natural variation between the plants, location in the plant or due to the inhibitor treatment (Lord et al. 2020). Many commonly used statistical tests, including the t-test, are sensitive to sample size and data distribution, so oversampling each biological replicate and therefore artificially inflating sample size can dramatically skew conclusions from statistical analyses and data that do not fit a normal distribution may need to be compared via alternative statistical tests. Best practices include clearly defining sample size in methods and figure legends, defining

sample size as the number of independent biological replicates, testing data for assumptions of common statistical tests (e.g., normality, equal variance), using appropriate statistical analyses, and plotting data in a transparent fashion (e.g., using a plot type that displays all data points along with summary statistics).

5.4 Figure/Results Presentation

While each journal will have individual requirements for figure preparation, several steps are universal when preparing microscopy figures for publication. Figure and movie legends must include essential information for interpretation, such as scale bars, time stamps, and calibration bars for any non-linear lookup tables (false-coloring of images). Figure legends should also contain clear information about the cell type and developmental stage observed, as well as an indication of whether images are single frame or a projection (e.g. a maximum intensity projection of a z-stack or sum projection of a time series). When direct comparisons are being made between wild type and mutant, or treatment and control, control and experimental images should be displayed in the same fashion.

While the complete list of factors that must be reported for any microscopy experiment can seem overwhelming, appropriate methods reporting facilitates research communication, experimental reproducibility, and data accessibility. Therefore, we urge authors and reviewers to make use of the reporting spreadsheet template provided here (**Supplementary Table 1**) and suggest that scientists collect this information as they conduct their experiments to ensure that microscopy methods are appropriately reported in any resulting publication. While reporting can be complex, regularly updating conventional or electronic lab notebooks through the entire process simplifies data analysis, data interpretation and manuscript preparation (Buckholt and Rulfs 2022).

Conclusion

Many factors are involved in obtaining robust and meaningful results when applying fluorescence imaging across diverse scientific questions in plant research. While not exhaustive, the goal of this primer was to bring attention to and provide a guide

through some of the most common challenges that arise in plant fluorescent imaging experiments from experimental design to publication. Many common pitfalls in plant imaging can be simply remedied through awareness and training. Ultimately, imaging data can be obtained in many different ways but depending on the experimental goal and how data were acquired, there can be limitations on meaningful interpretation and quantitative results due to lack of adequate documentation and reporting. More importantly, in an effort toward transparency and following FAIR principles we urge the plant science community to accelerate improvements in quality control, efficiency, reproducibility, data availability, and biological insights by adopting these best practices in plant fluorescence imaging.

Acknowledgements and Funding

The Plant Cell Atlas Initiative was funded by the National Science Foundation Research Coordination Network (Award # 2052590) to Dr. Seung Rhee. H.E.M. is the Canada Research Chair in Plant Cell Biology. Some imaging was conducted using instruments supported by Canada Foundation for Innovation and the Ontario Research Fund grants (38721) to H.E.M. This work was supported in part by the Natural Sciences and Engineering Research Council of Canada NSERC Discovery Grant (2020-05959) and an Ontario Early Researcher Award (ER21-16-256) to H.E.M. K.J.C acknowledges imaging support from the Advanced Bioimaging Laboratory (RRID:SCR_018951) at the Danforth Plant Science Center and usage of the Leica SP8-X confocal microscope acquired through an NSF Major Research Instrumentation grant (DBI-1337680) and the ZEISS Elyra 7 Super-Resolution Microscope acquired through an NSF Major Research Instrumentation grant (DBI-2018962). D.K. was supported by the Natural Sciences and Engineering Research Council of Canada NSERC Discovery Grant (RGPIN-2018-04897). G.D. acknowledges support in part through access to the UC Davis MCB Light Microscopy Core Facility and a NIH Shared Instrumentation grant (S10OD026702) for funding of the Zeiss 980 LSM and training and support by Dr. Thomas Wilkop.

Supplemental Data

All original raw microscope image data (Figs. 3, 5, 6, 7, 8, 9, Supplementary Figs. 3, 4 & 5) will be made available as a public repository at Zenodo upon publication (**10.5281/zenodo.14895059**).

References

Aaron, Jesse and Teng-Leong Chew. 2021. “A Guide to Accurate Reporting in Digital Image Processing – Can Anyone Reproduce Your Quantitative Analysis?” *Journal of Cell Science* 134(6).

Abramowitz, Mortimer and Michael Davidson. 2015. “Microscope Objectives - Immersion Media.” Retrieved (https://micro.magnet.fsu.edu/primer/anatomy/immersion.html).

Ast, Cindy, Jessica Foret, Luke M. Oltrogge, Roberto De Michele, Thomas J. Kleist, Cheng-Hsun Ho, and Wolf B. Frommer. 2017. “Ratiometric Matryoshka Biosensors from a Nested Cassette of Green- and Orange-Emitting Fluorescent Proteins.” *Nature Communications* 8(1):431.

Aswani, Kavita, Tushare Jinadasa, and Claire M. Brown. 2012. “Fluorescence Microscopy Light Sources.” *Microscopy Today* 20(4):22–28.

Baker, Ralph. 1984. “The Controlled Experiment in the Scientific Method with Special Emphasis on Biological Control.” *Phytopathology* 74(9):1019.

Balcerowicz, Martin, Kartika N. Shetty, and Alexander M. Jones. 2021. “Fluorescent Biosensors Illuminating Plant Hormone Research.” *Plant Physiology* 187(2):590–602.

Barbier de Reuille, Pierre, Anne-Lise Routier-Kierzkowska, Daniel Kierzkowski, George W. Bassel, Thierry Schüpbach, Gerardo Tauriello, Namrata Bajpai, Sören Strauss, Alain Weber, Annamaria Kiss, Agata Burian, Hugo Hofhuis, Aleksandra Sapala, Marcin Lipowczan, Maria B. Heimlicher, Sarah Robinson, Emmanuelle M. Bayer, Konrad Basler, Petros Koumoutsakos, Adrienne HK Roeder, Tinri Aegerter-Wilmsen, Naomi Nakayama, Miltos Tsiantis, Angela Hay, Dorota Kwiatkowska, Ioannis Xenarios, Cris Kuhlemeier, and Richard S. Smith. 2015. “MorphoGraphX: A Platform for Quantifying Morphogenesis in 4D.” *ELife* 4:e05864.

Baskin, Tobias I., Catherine H. Busby, Larry C. Fowke, Margaret Sammut, and Frank Gubler. 1992. “Improvements in Immunostaining Samples Embedded in Methacrylate: Localization of Microtubules and Other Antigens throughout

Developing Organs in Plants of Diverse Taxa." *Planta* 187(3):405–13.
Bassel, George W. and Richard S. Smith. 2016. "Quantifying Morphogenesis in Plants in 4D." *Current Opinion in Plant Biology* 29:87–94.
Bell, Karen, Steve Mitchell, Danae Paultre, Markus Posch, and Karl Oparka. 2013. "Correlative Imaging of Fluorescent Proteins in Resin-Embedded Plant Material 1." *Plant Physiology* 161(4):1595–1603.
Berg, R. Howard and Roger N. Beachy. 2008. "Fluorescent Protein Applications in Plants." Pp. 153–77 in *Methods Cell Bio*.
BINA. n.d. "Bioimaging North America - Metrology Suitcase." Retrieved (https://www.bioimagingnorthamerica.org/metrology-suitcase/).
Brown, Danielle L. 2017. "Bias in Image Analysis and Its Solution: Unbiased Stereology." *Journal of Toxicologic Pathology* 30(3):183–91.
Buckholt, Michael A. and Jill Rulfs. 2022. "Electronic Laboratory Notebook Use Supports Good Experimental Practice and Facilitates Data Sharing, Archiving and Analysis." Pp. 415–40 in *Trends in Teaching Experimentation in the Life Sciences. Contributions from Biology Education Research.*, edited by T. R. Pelaez, N.J., Gardner, S.M., Anderson. Springer, Cham.
Burley, Stephen K., Helen M. Berman, Charmi Bhikadiya, Chunxiao Bi, Li Chen, Luigi Di Costanzo, Cole Christie, Jose M. Duarte, Shuchismita Dutta, Zukang Feng, Sutapa Ghosh, David S. Goodsell, Rachel Kramer Green, Vladimir Guranovic, Dmytro Guzenko, Brian P. Hudson, Yuhe Liang, Robert Lowe, Ezra Peisach, Irina Periskova, Chris Randle, Alexander Rose, Monica Sekharan, Chenghua Shao, Yi-Ping Tao, Yana Valasatava, Maria Voigt, John Westbrook, Jasmine Young, Christine Zardecki, Marina Zhuravleva, Genji Kurisu, Haruki Nakamura, Yumiko Kengaku, Hasumi Cho, Junko Sato, Ju Yaen Kim, Yasuyo Ikegawa, Atsushi Nakagawa, Reiko Yamashita, Takahiro Kudou, Gert-Jan Bekker, Hirofumi Suzuki, Takeshi Iwata, Masashi Yokochi, Naohiro Kobayashi, Toshimichi Fujiwara, Sameer Velankar, Gerard J. Kleywegt, Stephen Anyango, David R. Armstrong, John M. Berrisford, Matthew J. Conroy, Jose M. Dana, Mandar Deshpande, Paul Gane, Romana Gáborová, Deepti Gupta, Aleksandras Gutmanas, Jaroslav Koča, Lora Mak, Saqib Mir, Abhik Mukhopadhyay, Nurul Nadzirin, Sreenath Nair, Ardan

Patwardhan, Typhaine Paysan-Lafosse, Lukas Pravda, Osman Salih, David Sehnal, Mihaly Varadi, Radka Vařeková, John L. Markley, Jeffrey C. Hoch, Pedro R. Romero, Kumaran Baskaran, Dimitri Maziuk, Eldon L. Ulrich, Jonathan R. Wedell, Hongyang Yao, Miron Livny, and Yannis E. Ioannidis. 2019. “Protein Data Bank: The Single Global Archive for 3D Macromolecular Structure Data.” *Nucleic Acids Research* 47(D1):D520–28.

Campbell, Robert E., Oded Tour, Amy E. Palmer, Paul A. Steinbach, Geoffrey S. Baird, David A. Zacharias, and Roger Y. Tsien. 2002. “A Monomeric Red Fluorescent Protein.” *Proceedings of the National Academy of Sciences* 99(12):7877–82.

Celler, Katherine, Miki Fujita, Eiko Kawamura, Chris Ambrose, Klaus Herburger, Andreas Holzinger, and Geoffrey O. Wasteneys. 2016. “Microtubules in Plant Cells: Strategies and Methods for Immunofluorescence, Transmission Electron Microscopy, and Live Cell Imaging.” Pp. 155–84 in.

Chow, Fabrizio, Eskandar Mohammad, and Heather E. McFarlane. 2025. “Protocol for Detecting Intracellular Aggregations in Arabidopsis Thaliana Cell Wall Mutants Using FM4-64 Staining.” *STAR Protocols* 6(1):103665.

Chu, Kevin L., Somnath Koley, Lauren M. Jenkins, Sally R. Bailey, Shrikaar Kambhampati, Kevin Foley, Jennifer J. Arp, Stewart A. Morley, Kirk J. Czymmek, Philip D. Bates, and Doug K. Allen. 2022. “Metabolic Flux Analysis of the Non-Transitory Starch Tradeoff for Lipid Production in Mature Tobacco Leaves.” *Metabolic Engineering* 69:231–48.

Clancy, B. and L. .. Cauller. 1998. “Reduction of Background Autofluorescence in Brain Sections Following Immersion in Sodium Borohydride.” *Journal of Neuroscience Methods* 83(2):97–102.

Clark, Natalie M., Elizabeth Hinde, Cara M. Winter, Adam P. Fisher, Giuseppe Crosti, Ikram Blilou, Enrico Gratton, Philip N. Benfey, and Rosangela Sozzani. 2016. “Tracking Transcription Factor Mobility and Interaction in Arabidopsis Roots with Fluorescence Correlation Spectroscopy.” *ELife* 5(JUN2016):1–25.

Colin, Leia, Raquel Martin-Arevalillo, Simone Bovio, Amélie Bauer, Teva Vernoux, Marie-Cecile Caillaud, Benoit Landrein, and Yvon Jaillais. 2022. “Imaging the Living Plant Cell: From Probes to Quantification.” *The Plant Cell* 34(1):247–72.

Collins, Tony J. 2006. “Mounting Media and Antifade Reagents.” *Microscopy Today* 14(1):34–39.

Conéjéro, Geneviève, Michel Noirot, Pascale Talamond, and Jean-Luc Verdeil. 2014. “Spectral Analysis Combined with Advanced Linear Unmixing Allows for Histolocalization of Phenolics in Leaves of Coffee Trees.” *Frontiers in Plant Science* 5(Feb):39.

Cox, Kevin L., Sarah A. Pardi, Lily O’Connor, Anastasiya Klebanovych, David Huss, Dmitri A. Nusinow, Blake C. Meyers, and Kirk J. Czymmek. 2025. “<scp>ExPOSE</Scp> : A Comprehensive Toolkit to Perform Expansion Microscopy in Plant Protoplast Systems.” *The Plant Journal* 121(5).

Cromey, Douglas W. 2010. “Avoiding Twisted Pixels: Ethical Guidelines for the Appropriate Use and Manipulation of Scientific Digital Images.” *Science and Engineering Ethics* 16(4):639–67.

Czymmek, K. J., M. L. Fogg, J. A. Sweigard, and S. Kang. 2004. “In Vivo Microscopy of Vascular Wilt Disease in Arabidposis Thaliana.” *Microscopy and Microanalysis* 10(SUPPL. 2).

Czymmek, Kirk J., Keith E. Duncan, and Howard Berg. 2023. “Realizing the Full Potential of Advanced Microscopy Approaches for Interrogating Plant-Microbe Interactions.” *Molecular Plant-Microbe Interactions®* 36(4):245–55.

Czymmek, Kirk J., Melissa Fogg, Deborah H. Powell, James Sweigard, Sook-Young Park, and Seogchan Kang. 2007. “In Vivo Time-Lapse Documentation Using Confocal and Multi-Photon Microscopy Reveals the Mechanisms of Invasion into the Arabidopsis Root Vascular System by Fusarium Oxysporum.” *Fungal Genetics and Biology* 44(10):1011–23.

Davidson, Michael E. Dailey; Sidney L. Shaw; Jason R. Swedlow; Paul D. Andrews; Matthias F. Langhorts; Michael W. 2024. “ZEISS Campus: Education in Microscopy and Digital Imaging.” Retrieved (https://zeiss-campus.magnet.fsu.edu/articles/livecellimaging/techniques.html).

Day, Kasey J., Patrick J. La Rivière, Talon Chandler, Vytas P. Bindokas, Nicola J. Ferrier, and Benjamin S. Glick. 2017. “Improved Deconvolution of Very Weak Confocal Signals.” *F1000Research* 6:787.

1096 Diel, Erin E., Jeff W. Lichtman, and Douglas S. Richardson. 2020. “Tutorial: Avoiding
1097 and Correcting Sample-Induced Spherical Aberration Artifacts in 3D Fluorescence
1098 Microscopy.” *Nature Protocols* 15(9):2773–84.
1099 Donaldson, Lloyd. 2020. “Autofluorescence in Plants.” *Molecules* 25(10):2393.
1100 Duncan, Keith E., Kirk J. Czymmek, Ni Jiang, August C. Thies, and Christopher N.
1101 Topp. 2022. “X-Ray Microscopy Enables Multiscale High-Resolution 3D Imaging of
1102 Plant Cells, Tissues, and Organs.” *Plant Physiology* 188(2):831–45.
1103 Duwé, Sam and Peter Dedecker. 2019. “Optimizing the Fluorescent Protein Toolbox
1104 and Its Use.” *Current Opinion in Biotechnology* 58:183–91.
1105 Dyachok, Julia, J. Alan Sparks, Fuqi Liao, Yuh-Shuh Wang, and Elison B. Blancaflor.
1106 2014. “Fluorescent Protein-based Reporters of the Actin Cytoskeleton in Living
1107 Plant Cells: Fluorophore Variant, Actin Binding Domain, and Promoter
1108 Considerations.” *Cytoskeleton* 71(5):311–27.
1109 Ebert, Berit, Carsten Rautengarten, Heather E. McFarlane, Thusitha Rupasinghe, Wei
1110 Zeng, Kristina Ford, Henrik V. Scheller, Antony Bacic, Ute Roessner, Staffan
1111 Persson, and Joshua L. Heazlewood. 2018. “A Golgi UDP-GlcNAc Transporter
1112 Delivers Substrates for N-Linked Glycans and Sphingolipids.” *Nature Plants*
1113 4(10):792–801.
1114 Engel, Benjamin D., Miroslava Schaffer, Luis Kuhn Cuellar, Elizabeth Villa, Jürgen M.
1115 Plitzko, and Wolfgang Baumeister. 2015. “Native Architecture of the
1116 Chlamydomonas Chloroplast Revealed by in Situ Cryo-Electron Tomography.”
1117 *ELife* 4:e04889.
1118 Fahlgren, Noah, Malia A. Gehan, and Ivan Baxter. 2015. “Lights, Camera, Action: High-
1119 Throughput Plant Phenotyping Is Ready for a Close-Up.” *Current Opinion in Plant*
1120 *Biology* 24:93–99.
1121 Fellers, Thomas J.; Davidson, Michael W. 2024. “Nikon Microscopy U - Coverslip
1122 Correction.” Retrieved (https://www.microscopyu.com/microscopy-basics/coverslip-
1123 correction).
1124 Foster, Erin D. and Ariel Deardorff. 2017. “Open Science Framework (OSF).” *Journal of*
1125 *the Medical Library Association* 105(2).
1126 Fujita, Miki, Regina Himmelspach, Juliet Ward, Angela Whittington, Nortrud Hasenbein,

Christine Liu, Thy T. Truong, Moira E. Galway, Shawn D. Mansfield, Charles H. Hocart, and Geoffrey O. Wasteneys. 2013. “The Anisotropy1 D604N Mutation in the Arabidopsis Cellulose Synthase1 Catalytic Domain Reduces Cell Wall Crystallinity and the Velocity of Cellulose Synthase Complexes.” *Plant Physiology* 162(1):74–85.

Galvan-Ampudia, Carlos S., Guillaume Cerutti, Jonathan Legrand, Géraldine Brunoud, Raquel Martin-Arevalillo, Romain Azais, Vincent Bayle, Steven Moussu, Christian Wenzl, Yvon Jaillais, Jan U. Lohmann, Christophe Godin, and Teva Vernoux. 2020. “Temporal Integration of Auxin Information for the Regulation of Patterning.” *ELife* 9:e55832.

Gaudreault, Nathalie. 2022. “Illumination Power, Stability, and Linearity Measurements for Confocal and Widefield Microscopes V2.” protocols.io. Retrieved (https://www.protocols.io/view/illumination-power-stability-and-linearity-measure-b68prhvn).

Geldner, Niko, Valérie Dénervaud-Tendon, Derek L. Hyman, Ulrike Mayer, York-Dieter Stierhof, and Joanne Chory. 2009. “Rapid, Combinatorial Analysis of Membrane Compartments in Intact Plants with a Multicolor Marker Set.” *The Plant Journal* 59(1):169–78.

Gilroy, Simon. 1997. “Fluorescence Microscopy of Living Plant Cells.” *Annual Review of Plant Physiology and Plant Molecular Biology* 48(1):165–90.

Le Gloanec, Constance, Andrea Gómez-Felipe, Viraj Alimchandani, Elvis Branchini, Amélie Bauer, Anne-Lise Routier-Kierzkowska, and Daniel Kierzkowski. 2024. “Modulation of Cell Differentiation and Growth Underlies the Shift from Bud Protection to Light Capture in Cauline Leaves.” *Plant Physiology* 196(2):1214–30.

Gómez-Felipe, Andrea, Elvis Branchini, Binghan Wang, Marco Marconi, Hana Bertrand-Rakusová, Teodora Stan, Jérôme Burkiewicz, Stefan de Folter, Anne-Lise Routier-Kierzkowska, Krzysztof Wabnik, and Daniel Kierzkowski. 2024. “Two Orthogonal Differentiation Gradients Locally Coordinate Fruit Morphogenesis.” *Nature Communications* 15(1):2912.

Goodwin, Paul C. 2007. “Evaluating Optical Aberration Using Fluorescent Microspheres: Methods, Analysis, and Corrective Actions.” Pp. 397–413 in

Methods Cell Bio.

Grefen, Christopher and Michael R. Blatt. 2012. “A 2in1 Cloning System Enables Ratiometric Bimolecular Fluorescence Complementation (RBiFC).” *BioTechniques* 53(5):311–14.

Guerin, Christopher J. 2023a. “Using Antibodies in Microscopy: A Guide to Immunohistochemistry. Part 1: Antibodies, Tissue Fixation, Embedding, and Sectioning.” *Microscopy Today* 31(2):26–31.

Guerin, Christopher J. 2023b. “Using Antibodies in Microscopy: A Guide to Immunohistochemistry. Part 2: IHC Staining Protocols.” *Microscopy Today* 31(3):34–39.

Halazonetis, Demetrios J. 2005. “What Do 8-Bit and 12-Bit Grayscale Mean and Which Should I Use When Scanning?” *American Journal of Orthodontics and Dentofacial Orthopedics* 127(3):387–88.

Hamant, Olivier, Marcus G. Heisler, Henrik Jönsson, Pawel Krupinski, Magalie Uyttewaal, Plamen Bokov, Francis Corson, Patrik Sahlin, Arezki Boudaoud, Elliot M. Meyerowitz, Yves Couder, and Jan Traas. 2008. “Developmental Patterning by Mechanical Signals in Arabidopsis.” *Science* 322(5908):1650–55.

Hardham, Adrienne R. 2012. “Confocal Microscopy in Plant–Pathogen Interactions Adrienne.” Pp. 295–309 in *Plant Fungal Pathogens: Methods and Protocols, Methods in Molecular Biology*. Vol. 835, edited by Melvin D. Bolton and Bart P.H.J. Thomma (eds.). Springer Science+Business Media.

Hartley, Matthew, Gerard J. Kleywegt, Ardan Patwardhan, Ugis Sarkans, Jason R. Swedlow, and Alvis Brazma. 2022. “The BioImage Archive – Building a Home for Life-Sciences Microscopy Data.” *Journal of Molecular Biology* 434(11):167505.

Haseloff, Jim. 1999. “Imaging Green Fluorescent Protein in Transgenic Plants.” *Imaging Living Cells* 362–94.

Heddleston, John M., Jesse S. Aaron, Satya Khuon, and Teng-Leong Chew. 2021. “A Guide to Accurate Reporting in Digital Image Acquisition – Can Anyone Replicate Your Microscopy Data?” *Journal of Cell Science* 134(6):jcs254144.

Hepler, Peter K. and Brian E. S. Gunning. 1998. “Confocal Fluorescence Microscopy of Plant Cells.” *Protoplasma* 201(3–4):121–57.

Hériché, Mathilde, Christine Arnould, Daniel Wipf, and Pierre-Emmanuel Courty. 2022. "Imaging Plant Tissues: Advances and Promising Clearing Practices." *Trends in Plant Science* 27(6):601–15.

Herud-Sikimić, Ole, Andre C. Stiel, Martina Kolb, Sooruban Shanmugaratnam, Kenneth W. Berendzen, Christian Feldhaus, Birte Höcker, and Gerd Jürgens. 2021. "A Biosensor for the Direct Visualization of Auxin." *Nature* 592(7856):768–72.

Hervieux, Nathan, Mathilde Dumond, Aleksandra Sapala, Anne-Lise Routier-Kierzkowska, Daniel Kierzkowski, Adrienne H. K. Roeder, Richard S. Smith, Arezki Boudaoud, and Olivier Hamant. 2016. "A Mechanical Feedback Restricts Sepal Growth and Shape in Arabidopsis." *Current Biology* 26(8):1019–28.

Hickey, Shane M., Ben Ung, Christie Bader, Robert Brooks, Joanna Lazniewska, Ian R. D. Johnson, Alexandra Sorvina, Jessica Logan, Carmela Martini, Courtney R. Moore, Litsa Karageorgos, Martin J. Sweetman, and Douglas A. Brooks. 2021. "Fluorescence Microscopy—An Outline of Hardware, Biological Handling, and Fluorophore Considerations." *Cells* 11(1):35.

Hobson, Chad M., Min Guo, Harshad D. Vishwasrao, Yicong Wu, Hari Shroff, and Teng-Leong Chew. 2022. "Practical Considerations for Quantitative Light Sheet Fluorescence Microscopy." *Nature Methods* 19(12):1538–49.

Hoffmann, Natalie, Eskandar Mohammad, and Heather E. McFarlane. 2024. "Disrupting Cell Wall Integrity Impacts Endomembrane Trafficking to Promote Secretion over Endocytic Trafficking" edited by M. Eggert Nielsen. *Journal of Experimental Botany* 75(12):3731–47.

Huynh, Jennie, Sara K. Hotton, Ron Chan, Yasra Syed, and James Thomson. 2022. "Evaluation of Novel Surfactants for Plant Transformation." *BMC Research Notes* 15(1):360.

Iudin, Andrii, Paul K. Korir, José Salavert-Torres, Gerard J. Kleywegt, and Ardan Patwardhan. 2016. "EMPIAR: A Public Archive for Raw Electron Microscopy Image Data." *Nature Methods* 13(5):387–88.

Iudin, Andrii, Paul K. Korir, Sriram Somasundharam, Simone Weyand, Cesare Cattavitello, Neli Fonseca, Osman Salih, Gerard J. Kleywegt, and Ardan Patwardhan. 2023. "EMPIAR: The Electron Microscopy Public Image Archive."

Nucleic Acids Research 51(D1):D1503–11.

Jacques, Eveline, Jean-Pierre Verbelen, and Kris Vissenberg. 2013. “Mechanical Stress in Arabidopsis Leaves Orients Microtubules in a 'continuous’ Supracellular Pattern.” *BMC Plant Biology* 13(1):163.

Jambor, Helena, Alberto Antonietti, Bradly Alicea, Tracy L. Audisio, Susann Auer, Vivek Bhardwaj, Steven J. Burgess, Iuliia Ferling, Małgorzata Anna Gazda, Luke H. Hoeppner, Vinodh Ilangovan, Hung Lo, Mischa Olson, Salem Yousef Mohamed, Sarvenaz Sarabipour, Aalok Varma, Kaivalya Walavalkar, Erin M. Wissink, and Tracey L. Weissgerber. 2021. “Creating Clear and Informative Image-Based Figures for Scientific Publications” edited by J. R. Swedlow. *PLOS Biology* 19(3):e3001161.

Jiang, Jiming. 2019. “Fluorescence in Situ Hybridization in Plants: Recent Developments and Future Applications.” *Chromosome Research* 27(3):153–65.

Jones, Kiersun, Dong Won Kim, Jean S. Park, and Chang Hyun Khang. 2016. “Live-Cell Fluorescence Imaging to Investigate the Dynamics of Plant Cell Death during Infection by the Rice Blast Fungus Magnaporthe Oryzae.” *BMC Plant Biology* 16(1):69.

Jonkman, James. 2020. “Rigor and Reproducibility in Confocal Fluorescence Microscopy.” *Cytometry Part A* 97(2):113–15.

Jonkman, James, Claire M. Brown, Graham D. Wright, Kurt I. Anderson, and Alison J. North. 2020. “Guidance for Quantitative Confocal Microscopy.” *Nature Protocols*.

Jonkman, James E. N., Jim Swoger, Holger Kress, Alexander Rohrbach, and Ernst H. K. Stelzer. 2003. “[18] Resolution in Optical Microscopy.” Pp. 416–46 in *Methods in Enzymology*, edited by G. Marriott and I. Parker. Academic Press.

Jost, Anna Payne-Tobin and Jennifer C. Waters. 2019. “Designing a Rigorous Microscopy Experiment: Validating Methods and Avoiding Bias.” *Journal of Cell Biology* 218(5):1452–66.

Kana, R., B. Sediva, and O. Prasil. 2023. “Microdomains Heterogeneity in the Thylakoid Membrane Proteins Visualized by Super-Resolution Microscopy.” *Photosynthetica* 61(SPECIAL ISSUE 2023-2):483–91.

Kao, Ping and Michael D. Nodine. 2021. “Application of Expansion Microscopy on

Developing Arabidopsis Seeds." Pp. 181–95 in.
Keller, H. Ernst. 1990. "Objective Lenses For Confocal Microscopy." Pp. 77–86 in *Handbook of Biological Confocal Microscopy*. Boston, MA: Springer US.
Kirby, A. R., A. P. Gunning, K. W. Waldron, V. J. Morris, and A. Ng. 1996. "Visualization of Plant Cell Walls by Atomic Force Microscopy." *Biophysical Journal* 70(3):1138–43.
Knapp, Elisabeth, Rosemary Flores, David Scheiblin, Shannon Modla, Kirk Czymmek, and Vidadi Yusibov. 2012. "A Cryohistological Protocol for Preparation of Large Plant Tissue Sections for Screening Intracellular Fluorescent Protein Expression." *BioTechniques* 52(1):31–37.
Komis, George, Olga Šamajová, Miroslav Ovečka, and Jozef Šamaj. 2015a. "Super-Resolution Microscopy in Plant Cell Imaging." *Trends in Plant Science* 20(12):834–43.
Komis, George, Olga Šamajová, Miroslav Ovečka, and Jozef Šamaj. 2015b. "Super-Resolution Microscopy in Plant Cell Imaging." *Trends in Plant Science* 20(12):834–43.
Krebs, Melanie, Katrin Held, Andreas Binder, Kenji Hashimoto, Griet Den Herder, Martin Parniske, Jörg Kudla, and Karin Schumacher. 2012. "FRET-Based Genetically Encoded Sensors Allow High-Resolution Live Cell Imaging of Ca 2+ Dynamics." *Plant Journal* 69(1):181–92.
Kurihara, Daisuke, Yoko Mizuta, Yoshikatsu Sato, and Tetsuya Higashiyama. 2015. "ClearSee: A Rapid Optical Clearing Reagent for Whole-Plant Fluorescence Imaging." *Development (Cambridge)* 142(23):4168–79.
Lambert, Talley J. 2019. "FPbase: A Community-Editable Fluorescent Protein Database." *Nature Methods* 16(4):277–78.
Lathe, Rahul S., Heather E. McFarlane, Christopher Kesten, Liu Wang, Ghazanfar Abbas Khan, Berit Ebert, Eduardo Antonio Ramírez-Rodríguez, Shuai Zheng, Niels Noord, Kristian Frandsen, Rishikesh P. Bhalerao, and Staffan Persson. 2024. "NKS1/ELMO4 Is an Integral Protein of a Pectin Synthesis Protein Complex and Maintains Golgi Morphology and Cell Adhesion in Arabidopsis." *Proceedings of the National Academy of Sciences* 121(15):e2321759121.

Lee, Jen-Yi and Maiko Kitaoka. 2018. “A Beginner’s Guide to Rigor and Reproducibility in Fluorescence Imaging Experiments” edited by D. G. Drubin. *Molecular Biology of the Cell* 29(13):1519–25.

Lee, Kieran J. D. and J. Paul Knox. 2014. “Resin Embedding, Sectioning, and Immunocytochemical Analyses of Plant Cell Walls in Hard Tissues.” *Methods in Molecular Biology* 1080:41–52.

Lee, Rachel M., Leanna R. Eisenman, Satya Khuon, Jesse S. Aaron, and Teng-Leong Chew. 2024. “Believing Is Seeing – the Deceptive Influence of Bias in Quantitative Microscopy.” *Journal of Cell Science* 137(1).

Leroux, Olivier. 2020. “Vibratome Sectioning of Plant Materials for (Immuno)Cytochemical Staining.” Pp. 339–50 in *The Plant Cell Wall. Methods in Molecular Biology*, edited by Z. Popper. New York, NY: Humana Press.

Leung, Bonnie O. and Keng C. Chou. 2011. “Review of Super-Resolution Fluorescence Microscopy for Biology.” *Applied Spectroscopy* 65(9):967–80.

Lichtman, Jeff W. and José-Angel Conchello. 2005. “Fluorescence Microscopy.” *Nature Methods* 2(12):910–19.

Lindeboom, Jelmer J., Masayoshi Nakamura, Anneke Hibbel, Kostya Shundyak, Ryan Gutierrez, Tijs Ketelaar, Anne Mie C. Emons, Bela M. Mulder, Viktor Kirik, and David W. Ehrhardt. 2013. “A Mechanism for Reorientation of Cortical Microtubule Arrays Driven by Microtubule Severing.” *Science* 342(6163).

Lipsitch, Marc, Eric Tchetgen Tchetgen, and Ted Cohen. 2010. “Negative Controls.” *Epidemiology* 21(3):383–88.

Lisenbee, Cayle S., Sheetal K. Karnik, and Richard N. Trelease. 2003. “Overexpression and Mislocalization of a Tail-Anchored GFP Redefines the Identity of Peroxisomal ER.” *Traffic* 4(7):491–501.

Littlejohn, George R., João D. Gouveia, Christoph Edner, Nicholas Smirnoff, and John Love. 2010. “Perfluorodecalin Enhances in Vivo Confocal Microscopy Resolution of Arabidopsis Thaliana Mesophyll.” *New Phytologist* 186(4):1018–25.

Littlejohn, George R., Jessica C. Mansfield, Jacqueline T. Christmas, Eleanor Witterick, Mark D. Fricker, Murray R. Grant, Nicholas Smirnoff, Richard M. Everson, Julian Moger, and John Love. 2014. “An Update: Improvements in Imaging

Perfluorocarbon-Mounted Plant Leaves with Implications for Studies of Plant Pathology, Physiology, Development and Cell Biology." *Frontiers in Plant Science* 5(APR):1–8.

Lord, Samuel J., Katrina B. Velle, R. Dyche Mullins, and Lillian K. Fritz-Laylin. 2020. "SuperPlots: Communicating Reproducibility and Variability in Cell Biology." *Journal of Cell Biology* 219(6):e202001064.

Mahmoudian, Jafar, Reza Hadavi, Mahmood Jeddi-Tehrani, Ahmad Reza Mahmoudi, Ali Ahmad Bayat, Elham Shaban, Mohtaram Vafakhah, Maryam Darzi, Majid Tarahomi, and Roya Ghods. 2011. "Comparison of the Photobleaching and Photostability Traits of Alexa Fluor 568- and Fluorescein Isothiocyanate-Conjugated Antibody." *Cell Journal* 13(3):169–72.

Malabadi, Ravindra B., Jaime A. Teixeira Da Silva, and • K Nataraja. 2008. "Transgenic Plant Journal Green Fluorescent Protein in the Genetic Transformation of Plants." *Transgenic Plant Journal* 2(2):86–109.

Marion, Jessica, Romain Le Bars, Béatrice Satiat-Jeunemaitre, and Claire Boulogne. 2017. "Optimizing CLEM Protocols for Plants Cells: GMA Embedding and Cryosections as Alternatives for Preservation of GFP Fluorescence in Arabidopsis Roots." *Journal of Structural Biology* 198(3):196–202.

Marqués, Guillermo, Thomas Pengo, and Mark A. Sanders. 2020. "Imaging Methods Are Vastly Underreported in Biomedical Research." *ELife* 9.

Marques, Patricia, John Strong, Tom Strader, and Ru-ching Hsia. 2018. "Optimization of Automated Immuno EM for Both Pre- and Post-Embedding Labeling." *Microscopy and Microanalysis* 24(S1):1300–1301.

Martin, Cathie and Mike Blatt. 2013. "Manipulation and Misconduct in the Handling of Image Data." *The Plant Cell* 25(9):3147–48.

McNally, James G., Tatiana Karpova, John Cooper, and José Angel Conchello. 1999. "Three-Dimensional Imaging by Deconvolution Microscopy." *Methods* 19(3):373–85.

McNamara, George. 2024. "Fluorophores -Table." Retrieved (https://www.geomcnamara.com/fluorophore-table).

Mizuta, Yoko. 2021. "Advances in Two-Photon Imaging in Plants." *Plant and Cell*

Physiology 62(8):1224–30.

Monshausen, Gabriele B., Mark A. Messerli, and Simon Gilroy. 2008. “Imaging of the Yellow Cameleon 3.6 Indicator Reveals That Elevations in Cytosolic Ca2+ Follow Oscillating Increases in Growth in Root Hairs of Arabidopsis.” *Plant Physiology* 147(4):1690–98.

Montero Llopis, Paula, Rebecca A. Senft, Tim J. Ross-Elliott, Ryan Stephansky, Daniel P. Keeley, Preman Koshar, Guillermo Marqués, Ya-Sheng Gao, Benjamin R. Carlson, Thomas Pengo, Mark A. Sanders, Lisa A. Cameron, and Michelle S. Itano. 2021. “Best Practices and Tools for Reporting Reproducible Fluorescence Microscopy Methods.” *Nature Methods* 18(12):1463–76.

Moore, Ian and Angus Murphy. 2009. “Validating the Location of Fluorescent Protein Fusions in the Endomembrane System.” *The Plant Cell* 21(6):1632–36.

Munafò, Marcus R., Brian A. Nosek, Dorothy V. M. Bishop, Katherine S. Button, Christopher D. Chambers, Nathalie Percie du Sert, Uri Simonsohn, Eric-Jan Wagenmakers, Jennifer J. Ware, and John P. A. Ioannidis. 2017. “A Manifesto for Reproducible Science.” *Nature Human Behaviour* 1(1):0021.

Nebenführ, Andreas, Larry A. Gallagher, Terri G. Dunahay, Jennifer A. Frohlick, Anna M. Mazurkiewicz, Janet B. Meehl, and L. Andrew Staehelin. 1999. “Stop-and-Go Movements of Plant Golgi Stacks Are Mediated by the Acto-Myosin System.” *Plant Physiology* 121(4):1127–41.

Nelson, Brook K., Xue Cai, and Andreas Nebenführ. 2007. “A Multicolored Set of in Vivo Organelle Markers for Co-localization Studies in Arabidopsis and Other Plants.” *The Plant Journal* 51(6):1126–36.

Nelson, Glyn. 2022. “Monitoring the Point Spread Function for Quality Control of Confocal Microscopes V1.”

Noble, Elizabeth, Sunil Kumar, Frederik G. Görlitz, Chris Stain, Chris Dunsby, and Paul M. W. French. 2017. “In Vivo Label-Free Mapping of the Effect of a Photosystem II Inhibiting Herbicide in Plants Using Chlorophyll Fluorescence Lifetime.” *Plant Methods* 13(1):1–16.

North, Alison J. 2006. “Seeing Is Believing? A Beginners’ Guide to Practical Pitfalls in Image Acquisition.” *Journal of Cell Biology* 172(1):9–18.

Nybo, Kristie. 2012. “GFP Imaging in Fixed Cells.” *BioTechniques* 52(6):359–60.
Ono, M., T. Murakami, A. Kudo, M. Isshiki, H. Sawada, and A. Segawa. 2001. “Quantitative Comparison of Anti-Fading Mounting Media for Confocal Laser Scanning Microscopy.” *Journal of Histochemistry & Cytochemistry* 49(3):305–11.
Oreopoulos, John, Richard Berman, and Mark Browne. 2014. “Spinning-Disk Confocal Microscopy.” Pp. 123:153-175 in *Methods Cell Bio*.
Otegui, Marisa S. and Jannice G. Pennington. 2019. “Electron Tomography in Plant Cell Biology.” *Microscopy* 68(1):69–79.
Ovečka, Miroslav, Jiří Sojka, Michaela Tichá, George Komis, Jasim Basheer, Cintia Marchetti, Olga Šamajová, Lenka Kuběnová, and Jozef Šamaj. 2022. “Imaging Plant Cells and Organs with Light-Sheet and Super-Resolution Microscopy.” *Plant Physiology* 188(2):683–702.
Ovečka, Miroslav, Daniel von Wangenheim, Pavel Tomančák, Olga Šamajová, George Komis, and Jozef Šamaj. 2018. “Multiscale Imaging of Plant Development by Light-Sheet Fluorescence Microscopy.” *Nature Plants* 4(9):639–50.
Pawley, James B. 2006. “Points, Pixels, and Gray Levels: Digitizing Image Data.” Pp. 59–79 in *Handbook Of Biological Confocal Microscopy*. Boston, MA: Springer US.
Pawley, Jim. 2000. “The 39 Steps: A Cautionary Tale of Quantitative 3-D Fluorescence Microscopy.” *BioTechniques* 28(5):884–87.
Piccinini, Luca, Fabien Nirina Ramamonjy, and Robertas Ursache. 2024. “Imaging Plant Cell Walls Using Fluorescent Stains: The Beauty Is in the Details.” *Journal of Microscopy* 295(2):102–20.
Piña, Ricardo, Alma I. Santos-Díaz, Erika Orta-Salazar, Azucena Ruth Aguilar-Vazquez, Carola A. Mantellero, Isabel Acosta-Galeana, Argel Estrada-Mondragon, Mara Prior-Gonzalez, Jadir Isai Martinez-Cruz, and Abraham Rosas-Arellano. 2022. “Ten Approaches That Improve Immunostaining: A Review of the Latest Advances for the Optimization of Immunofluorescence.” *International Journal of Molecular Sciences* 23(3):1426.
Piovesan, Agnese, Valérie Vancauwenberghe, Tim Van De Looverbosch, Pieter Verboven, and Bart Nicolaï. 2021. “X-Ray Computed Tomography for 3D Plant Imaging.” *Trends in Plant Science* 26(11):1171–85.

1406 Prieto, Pilar, Graham Moore, and Peter Shaw. 2007. “Fluorescence in Situ Hybridization
1407 on Vibratome Sections of Plant Tissues.” *Nature Protocols* 2(7):1831–38.
1408 Prunet, Nathanaël, Thomas P. Jack, and Elliot M. Meyerowitz. 2016. “Live Confocal
1409 Imaging of Arabidopsis Flower Buds.” *Developmental Biology* 419(1):114–20.
1410 Russ, John C. 2006. *The Image Processing Handbook*. edited by J. C. Russ. Boca
1411 Raton: CRC Press.
1412 Sakamoto, Yuki, Anna Ishimoto, Yuuki Sakai, Moeko Sato, Ryuichi Nishihama, Konami
1413 Abe, Yoshitake Sano, Teiichi Furuichi, Hiroyuki Tsuji, Takayuki Kohchi, and
1414 Sachihiro Matsunaga. 2022. “Improved Clearing Method Contributes to Deep
1415 Imaging of Plant Organs.” *Communications Biology* 5(1):12.
1416 Samalova, Marketa, Mark Fricker, and Ian Moore. 2006. “Ratiometric Fluorescence-
1417 Imaging Assays of Plant Membrane Traffic Using Polyproteins.” *Traffic* 7(12):1701–
1418 23.
1419 Sawchuk, Megan G., Philip Head, Tyler J. Donner, and Enrico Scarpella. 2007. “Time-
1420 lapse Imaging of Arabidopsis Leaf Development Shows Dynamic Patterns of
1421 Procambium Formation.” *New Phytologist* 176(3):560–71.
1422 Scheuring, David, Elena A. Minina, Falco Krueger, Upendo Lupanga, Melanie Krebs,
1423 and Karin Schumacher. 2024. “Light at the End of the Tunnel: FRAP Assays
1424 Combined with Super Resolution Microscopy Confirm the Presence of a Tubular
1425 Vacuole Network in Meristematic Plant Cells.” *The Plant Cell* 36(11):4683–91.
1426 Schindelin, Johannes, Ignacio Arganda-Carreras, Erwin Frise, Verena Kaynig, Mark
1427 Longair, Tobias Pietzsch, Stephan Preibisch, Curtis Rueden, Stephan Saalfeld,
1428 Benjamin Schmid, Jean-Yves Tinevez, Daniel James White, Volker Hartenstein,
1429 Kevin Eliceiri, Pavel Tomancak, and Albert Cardona. 2012. “Fiji: An Open-Source
1430 Platform for Biological-Image Analysis.” *Nature Methods* 9(7):676–82.
1431 Schmied, Christopher, Michael S. Nelson, Sergiy Avilov, Gert-Jan Bakker, Cristina
1432 Bertocchi, Johanna Bischof, Ulrike Boehm, Jan Brocher, Mariana T. Carvalho,
1433 Catalin Chiritescu, Jana Christopher, Beth A. Cimini, Eduardo Conde-Sousa,
1434 Michael Ebner, Rupert Ecker, Kevin Eliceiri, Julia Fernandez-Rodriguez, Nathalie
1435 Gaudreault, Laurent Gelman, David Grunwald, Tingting Gu, Nadia Halidi, Mathias
1436 Hammer, Matthew Hartley, Marie Held, Florian Jug, Varun Kapoor, Ayse Aslihan

Koksoy, Judith Lacoste, Sylvia Le Dévédec, Sylvie Le Guyader, Penghuan Liu, Gabriel G. Martins, Aastha Mathur, Kota Miura, Paula Montero Llopis, Roland Nitschke, Alison North, Adam C. Parslow, Alex Payne-Dwyer, Laure Plantard, Rizwan Ali, Britta Schroth-Diez, Lucas Schütz, Ryan T. Scott, Arne Seitz, Olaf Selchow, Ved P. Sharma, Martin Spitaler, Sathya Srinivasan, Caterina Strambio-De-Castillia, Douglas Taatjes, Christian Tischer, and Helena Klara Jambor. 2024. "Community-Developed Checklists for Publishing Images and Image Analyses." *Nature Methods* 21(2):170–81.

Schneider, René, David W. Ehrhardt, Elliot M. Meyerowitz, and Arun Sampathkumar. 2022. "Tethering of Cellulose Synthase to Microtubules Dampens Mechano-Induced Cytoskeletal Organization in Arabidopsis Pavement Cells." *Nature Plants* 8(9):1064–73.

Schubert, Veit. 2017. "Super-Resolution Microscopy - Applications in Plant Cell Research." *Frontiers in Plant Science* 8(April):1–12.

Scipioni, L., L. Lanzanó, A. Diaspro, and E. Gratton. 2018. "Comprehensive Correlation Analysis for Super-Resolution Dynamic Fingerprinting of Cellular Compartments Using the Zeiss Airyscan Detector." *Nature Communications* 9(1):5120.

Segami, Shoji, Sachi Makino, Ai Miyake, Mariko Asaoka, and Masayoshi Maeshima. 2014. "Dynamics of Vacuoles and H+-Pyrophosphatase Visualized by Monomeric Green Fluorescent Protein in Arabidopsis : Artifactual Bulbs and Native Intravacuolar Spherical Structures." *The Plant Cell* 26(8):3416–34.

Shaner, Nathan C., Gerard G. Lambert, Andrew Chammas, Yuhui Ni, Paula J. Cranfill, Michelle A. Baird, Brittney R. Sell, John R. Allen, Richard N. Day, Maria Israelsson, Michael W. Davidson, and Jiwu Wang. 2013. "A Bright Monomeric Green Fluorescent Protein Derived from Branchiostoma Lanceolatum." *Nature Methods* 10(5):407–9.

Shaw, Sidney L. and David W. Ehrhardt. 2013. "Smaller, Faster, Brighter: Advances in Optical Imaging of Living Plant Cells." *Annual Review of Plant Biology* 64(1):351–75.

Shimamura, Masaki. 2015. "Whole-Mount Immunofluorescence Staining of Plant Cells and Tissues." Pp. 181–96 in *Plant Microtechniques and Protocols*. Cham: Springer

International Publishing.
Sicilia, Miguel-Angel, Elena García-Barriocanal, and Salvador Sánchez-Alonso. 2017. "Community Curation in Open Dataset Repositories: Insights from Zenodo." *Procedia Computer Science* 106:54–60.
Silveira, Sylvia R., Constance Le Gloanec, Andrea Gómez-Felipe, Anne-Lise Routier-Kierzkowska, and Daniel Kierzkowski. 2022. "Live-Imaging Provides an Atlas of Cellular Growth Dynamics in the Stamen." *Plant Physiology* 188(2):769–81.
SpectraViewer, Thermofisher Fluorescence. 2024. "Thermofisher Fluorescence SpectraViewer." Retrieved (https://www.thermofisher.com/order/fluorescence-spectraviewer/#!/).
Spring, Kenneth R. 2001. "Detectors for Fluorescence Microscopy." Pp. 40–52 in *Methods in Cellular Imaging*. New York, NY: Springer New York.
Staudt, Thorsten and Stefan W. Hell. 2008. "2,2-Tde." *Microscopy Research and Technique* 71(2):146–57.
Stewart, Jr. 2001. "The Utility of Green Fluorescent Protein in Transgenic Plants." *Plant Cell Reports* 20(5):376–82.
Stirling, David R., Madison J. Swain-Bowden, Alice M. Lucas, Anne E. Carpenter, Beth A. Cimini, and Allen Goodman. 2021. "CellProfiler 4: Improvements in Speed, Utility and Usability." *BMC Bioinformatics* 22(1):433.
Strauss, Sören, Adam Runions, Brendan Lane, Dennis Eschweiler, Namrata Bajpai, Nicola Trozzi, Anne-Lise Routier-Kierzkowska, Saiko Yoshida, Sylvia Rodrigues da Silveira, Athul Vijayan, Rachele Tofanelli, Mateusz Majda, Emillie Echevin, Constance Le Gloanec, Hana Bertrand-Rakusova, Milad Adibi, Kay Schneitz, George W. Bassel, Daniel Kierzkowski, Johannes Stegmaier, Miltos Tsiantis, and Richard S. Smith. 2022. "Using Positional Information to Provide Context for Biological Image Analysis with MorphoGraphX 2.0." *ELife* 11(e72601).
Swedlow, Jason R. 2007. "Quantitative Fluorescence Microscopy and Image Deconvolution." *Methods Cell Biol.* 81:447–65.
Sydor, Andrew M., Kirk J. Czymmek, Elias M. Puchner, and Vito Mennella. 2015. "Super-Resolution Microscopy: From Single Molecules to Supramolecular Assemblies." *Trends in Cell Biology* 25(12):730–48.

Tanz, Sandra K., Ian Castleden, Ian D. Small, and A. Harvey Millar. 2013. “Fluorescent Protein Tagging as a Tool to Define the Subcellular Distribution of Proteins in Plants.” *Frontiers in Plant Science* 4.

Tirichine, Lela, Philippe Andrey, Eric Biot, Yves Maurin, and Valérie Gaudin. 2009. “3D Fluorescent in Situ Hybridization Using Arabidopsis Leaf Cryosections and Isolated Nuclei.” *Plant Methods* 5(1):1–7.

Torday, John S. and František Baluška. 2019. “Why Control an Experiment?” *EMBO Reports* 20(10):e49110.

Truernit, Elisabeth, Hélène Bauby, Bertrand Dubreucq, Olivier Grandjean, John Runions, Julien Barthélémy, and Jean-Christophe Palauqui. 2008. “High-Resolution Whole-Mount Imaging of Three-Dimensional Tissue Organization and Gene Expression Enables the Study of Phloem Development and Structure in Arabidopsis.” *The Plant Cell* 20(6):1494–1503.

Truernit, Elisabeth and Jim Haseloff. 2008. “A Simple Way to Identify Non-Viable Cells within Living Plant Tissue Using Confocal Microscopy.” *Plant Methods* 4(1):15.

Ueda, Haruko, Etsuo Yokota, Natsumaro Kutsuna, Tomoo Shimada, Kentaro Tamura, Teruo Shimmen, Seiichiro Hasezawa, Valerian V. Dolja, and Ikuko Hara-Nishimura. 2010. “Myosin-Dependent Endoplasmic Reticulum Motility and F-Actin Organization in Plant Cells.” *Proceedings of the National Academy of Sciences* 107(15):6894–99.

Verbančič, Jana, Jenny Jiahui Huang, and Heather E. McFarlane. 2021. “Analysis of Cellulose Synthase Activity in Arabidopsis Using Spinning Disk Microscopy.” *STAR Protocols* 2(4):100863.

Voss, Ute, Antoine Larrieu, and Darren M. Wells. 2013. “From Jellyfish to Biosensors: The Use of Fluorescent Proteins in Plants.” *The International Journal of Developmental Biology* 57(6-7–8):525–33.

Waadt, Rainer and Jörg Kudla. 2008. “In Planta Visualization of Protein Interactions Using Bimolecular Fluorescence Complementation (BiFC).” *Cold Spring Harbor Protocols* 2008(4):pdb.prot4995.

Wan, Yinglang, William M. Ash, Lusheng Fan, Huaiqin Hao, Myung K. Kim, and Jinxing Lin. 2011. “Variable-Angle Total Internal Reflection Fluorescence Microscopy of

Intact Cells of Arabidopsis Thaliana." *Plant Methods* 7(1):27.

Wang, Binghan, Amélie Bauer, Andrea Gómez-Felipe, Sylvia Silveira, and Daniel Kierzkowski. 2025. "Confocal Live Imaging of Reproductive Organs Development in Arabidopsis." *Bio-Protocol* 15(1364).

Wang, Hanchen, Tianfan Fu, Yuanqi Du, Wenhao Gao, Kexin Huang, Ziming Liu, Payal Chandak, Shengchao Liu, Peter Van Katwyk, Andreea Deac, Anima Anandkumar, Karianne Bergen, Carla P. Gomes, Shirley Ho, Pushmeet Kohli, Joan Lasenby, Jure Leskovec, Tie-Yan Liu, Arjun Manrai, Debora Marks, Bharath Ramsundar, Le Song, Jimeng Sun, Jian Tang, Petar Veličković, Max Welling, Linfeng Zhang, Connor W. Coley, Yoshua Bengio, and Marinka Zitnik. 2023. "Scientific Discovery in the Age of Artificial Intelligence." *Nature* 620(7972):47–60.

Wang, Jie, Evelien Mylle, Alexander Johnson, Nienke Besbrugge, Geert De Jaeger, Jiří Friml, Roman Pleskot, and Daniel Van Damme. 2020. "High Temporal Resolution Reveals Simultaneous Plasma Membrane Recruitment of TPLATE Complex Subunits." *Plant Physiology* 183(3):986–97.

Wang, Yuh-Shuh, Cheol-Min Yoo, and Elison B. Blancaflor. 2008. "Improved Imaging of Actin Filaments in Transgenic Arabidopsis Plants Expressing a Green Fluorescent Protein Fusion to the C- and N-termini of the Fimbrin Actin-binding Domain 2." *New Phytologist* 177(2):525–36.

von Wangenheim, Daniel, Robert Hauschild, Matyáš Fendrych, Vanessa Barone, Eva Benková, and Jiří Friml. 2017. "Live Tracking of Moving Samples in Confocal Microscopy for Vertically Grown Roots." *ELife* 6(e26792).

Waters, Jennifer C. 2009. "Accuracy and Precision in Quantitative Fluorescence Microscopy." *Journal of Cell Biology* 185(7):1135–48.

Wernersson, Erik, Eleni Gelali, Gabriele Girelli, Su Wang, David Castillo, Christoffer Mattsson Langseth, Quentin Verron, Huy Q. Nguyen, Shyamtanu Chattoraj, Anna Martinez Casals, Hans Blom, Emma Lundberg, Mats Nilsson, Marc A. Marti-Renom, Chao-ting Wu, Nicola Crosetto, and Magda Bienko. 2024. "Deconwolf Enables High-Performance Deconvolution of Widefield Fluorescence Microscopy Images." *Nature Methods* 21(7):1245–56.

Westbrook, John D., Jasmine Y. Young, Chenghua Shao, Zukang Feng, Vladimir

Guranovic, Catherine L. Lawson, Brinda Vallat, Paul D. Adams, John M. Berrisford, Gerard Bricogne, Kay Diederichs, Robbie P. Joosten, Peter Keller, Nigel W. Moriarty, Oleg V. Sobolev, Sameer Velankar, Clemens Vonrhein, David G. Waterman, Genji Kurisu, Helen M. Berman, Stephen K. Burley, and Ezra Peisach. 2022. “PDBx/MmCIF Ecosystem: Foundational Semantic Tools for Structural Biology.” *Journal of Molecular Biology* 434(11):167599.

Wickramanayake, Janithri S. and Kirk J. Czymmek. 2023. “A Conventional Fixation Volume Electron Microscopy Protocol for Plants.” Pp. 83–99 in *Methods in Cell Biology*, edited by K. Narayan, L. Collinson, and P. Verkade. Academic Press.

Wightman, Raymond. 2022. “An Overview of Cryo-Scanning Electron Microscopy Techniques for Plant Imaging.” *Plants* 11(9).

Wilkinson, Mark D., Michel Dumontier, IJsbrand Jan Aalbersberg, Gabrielle Appleton, Myles Axton, Arie Baak, Niklas Blomberg, Jan-Willem Boiten, Luiz Bonino da Silva Santos, Philip E. Bourne, Jildau Bouwman, Anthony J. Brookes, Tim Clark, Mercè Crosas, Ingrid Dillo, Olivier Dumon, Scott Edmunds, Chris T. Evelo, Richard Finkers, Alejandra Gonzalez-Beltran, Alasdair J. G. Gray, Paul Groth, Carole Goble, Jeffrey S. Grethe, Jaap Heringa, Peter A. .. ’t Hoen, Rob Hooft, Tobias Kuhn, Ruben Kok, Joost Kok, Scott J. Lusher, Maryann E. Martone, Albert Mons, Abel L. Packer, Bengt Persson, Philippe Rocca-Serra, Marco Roos, Rene van Schaik, Susanna-Assunta Sansone, Erik Schultes, Thierry Sengstag, Ted Slater, George Strawn, Morris A. Swertz, Mark Thompson, Johan van der Lei, Erik van Mulligen, Jan Velterop, Andra Waagmeester, Peter Wittenburg, Katherine Wolstencroft, Jun Zhao, and Barend Mons. 2016. “The FAIR Guiding Principles for Scientific Data Management and Stewardship.” *Scientific Data* 3(1):160018.

Wilson, Sarah M. and Antony Bacic. 2012. “Preparation of Plant Cells for Transmission Electron Microscopy to Optimize Immunogold Labeling of Carbohydrate and Protein Epitopes.” *Nature Protocols* 7(9):1716–27.

Wu, Qingyu, Anding Luo, Tara Zadrozny, Anne Sylvester, and Dave Jackson. 2013. “Fluorescent Protein Marker Lines in Maize: Generation and Applications.” *International Journal of Developmental Biology* 57(6–8):535–43.

Yoshida, Shawn R., Barun K. Maity, and Shasha Chong. 2023. “Visualizing Protein

Localizations in Fixed Cells: Caveats and the Underlying Mechanisms." *The Journal of Physical Chemistry B* 127(19):4165–73.

Yu, Hye Young, Jeong Ah Seo, Jung Eun Kim, Kap Hoon Han, Won Bo Shim, Sung Hwan Yun, and Yin Won Lee. 2008. "Functional Analyses of Heterotrimeric G Protein Gα and Gβ Subunits in Gibberella Zeae." *Microbiology* 154(2):392–401.

Zhao, Huimin, Zilong Tan, Xuejing Wen, and Yucheng Wang. 2017. "An Improved Syringe Agroinfiltration Protocol to Enhance Transformation Efficiency by Combinative Use of 5-Azacytidine, Ascorbate Acid and Tween-20." *Plants* 6(1):9.

Zhou, Rudy, Han Liu, Tao Ju, and Ram Dixit. 2020. "Quantifying the Polymerization Dynamics of Plant Cortical Microtubules Using Kymograph Analysis." Pp. 160:281-293 in *Methods Cell Bio*.

Zhu, Mingyuan, Weiwei Chen, Vincent Mirabet, Lilan Hong, Simone Bovio, Soeren Strauss, Erich M. Schwarz, Satoru Tsugawa, Zhou Wang, Richard S. Smith, Chun-Biu Li, Olivier Hamant, Arezki Boudaoud, and Adrienne H. K. Roeder. 2020. "Robust Organ Size Requires Robust Timing of Initiation Orchestrated by Focused Auxin and Cytokinin Signalling." *Nature Plants* 6(6):686–98.

Zimmermann, Timo, Joanne Marrison, Karen Hogg, and Peter O'Toole. 2014. "Clearing Up the Signal: Spectral Imaging and Linear Unmixing in Fluorescence Microscopy." Pp. 129–48 in *Confocal Microscopy*, edited by Steven Paddock. New York, NY: Humana Press.

Zou, Yuchen, Weiwei Tang, and Bin Li. 2024. "Exploring Natural Product Biosynthesis in Plants with Mass Spectrometry Imaging." *Trends in Plant Science* (Sep 27).

1623
1624
1625
1626
1627
1628
1629
1630
1631
1632
1633
1634
1635
1636
1637
1638
1639
1640
1641
1642
1643
1644
1645
1646
1647
1648
1649
1650
1651
1652
1653

Figure 1

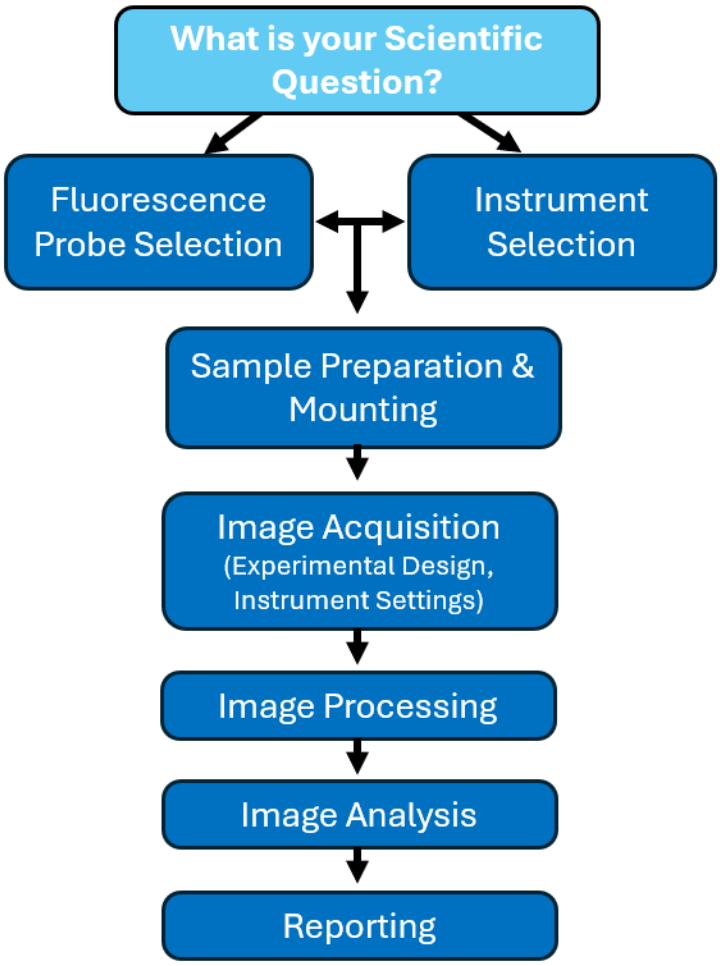

Figure 1: Key steps to imaging experiment workflow. 1) Consider Fluorescence Probe and Instrument Selection which are often interdependent and based on resource availability. 2) Select appropriate Sample Preparation & Mounting conditions. 3) Image Acquisition includes appropriate experimental design (e.g., controls) and instrument settings to obtain meaningful qualitative and/or quantitative results. Multiple imaging modalities and platforms may be useful to answer different aspects of a scientific question and the experiment setup may need to be refined depending on preliminary results. 4) Image Processing (if necessary) with documentation may be performed to facilitate visualization and/or quantification of target features, while 5) Image Analysis will translate image data into measurable quantitative comparisons of results. 6) Reporting includes disclosure of any essential parameters to document these steps for reproducibility,

peer review and reader interpretation. Note that this workflow is meant to provide a useful and logical framework but sometimes workflow order may not necessarily be as linear or rigid as portrayed, especially when troubleshooting.

Figure 2

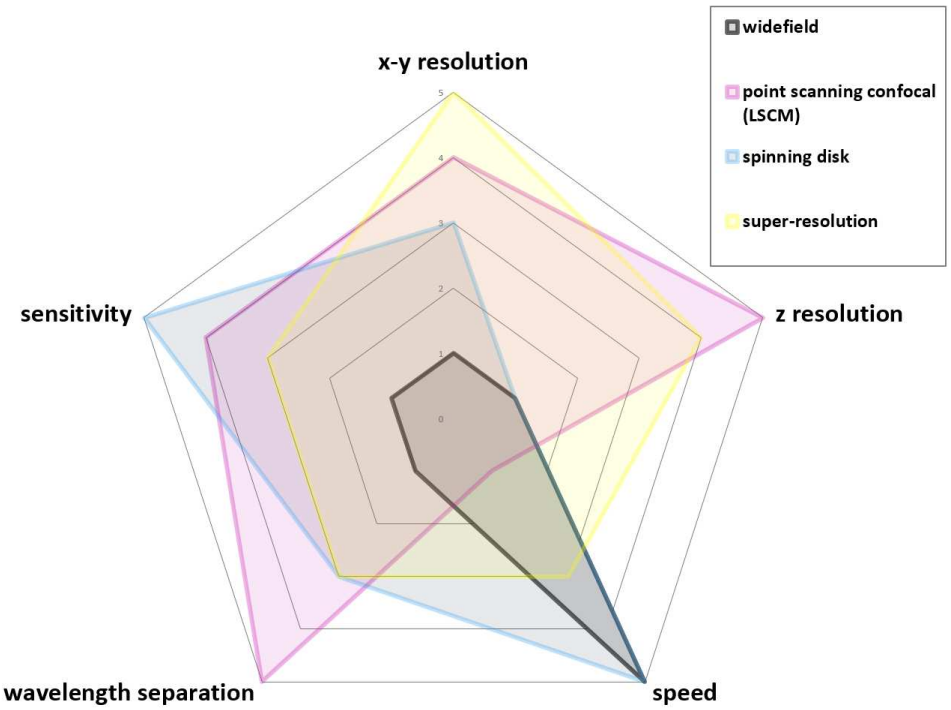

Figure 2: Dimensions of fluorescent imaging (and trade-offs). Selection of the optimal imaging platform depends on experimental goals. Super-resolution microscopy followed by point scanning confocal microscopy (aka LSCM) provide the greatest lateral (x-y) resolution, while spinning disk and widefield microscopy have the best speed for capturing dynamic events. Other criteria of note are the high signal collection efficiency (sensitivity) of spinning disk and the best z-resolution and wavelength separation with LSCM systems. Wavelength separation is best with spectral detection (more common in point scanning confocal microscopes) versus filter-based systems typically used in widefield and spinning disk systems. All platforms can be used for many plant imaging experiments, but some will perform better than others for certain tasks where resolution, dynamics, and/or spectral separation are critical. Note that this is a generalized chart and the exact proportional difference in each dimension is dependent upon the microscope setup and specific technique employed.

Figure 3

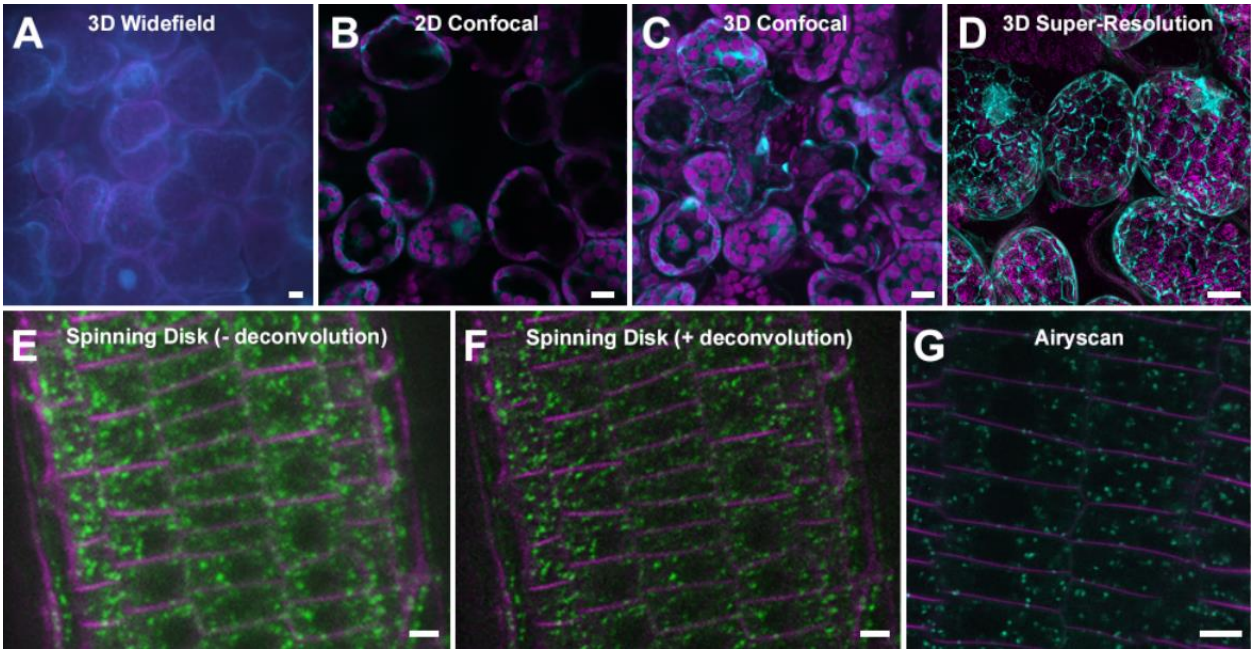

Figure 3. Plant leaf and root imaging comparing common fluorescence imaging modes. (A-D) A comparison of image contrast and detail with cytoplasmic expression of untagged CFP (cyan) and chlorophyll autofluorescence (magenta) in *N. benthamiana* leaf mesophyll cells. (A) 3D Widefield microscopy (z-stack maximum intensity projection) exhibited the lowest contrast while a single 2D optical section (B) and 3D confocal z-stack maximum intensity projection (C) showed increased contrast and cellular detail, while (D) 3D super-resolution (z-stack maximum intensity projection) provided the greatest cellular detail (resolution). (E-G) *A. thaliana* root division zone cell imaging of membrane stain, FM4-64 (magenta) and Syntaxin of Plants 61 CFP-SYP61 (green) comparing signal-to-noise, contrast and cellular detail from 3i spinning disk without (E) and with (F) deconvolution to ZEISS LSM980 Airyscan imaging (G); full details of the microscope hardware, software, and imaging setup for this and all other figures are supplied in Supplementary Table 1. Scale bars A-D = 10 µm, E-G = 5 µm.

Figure 4

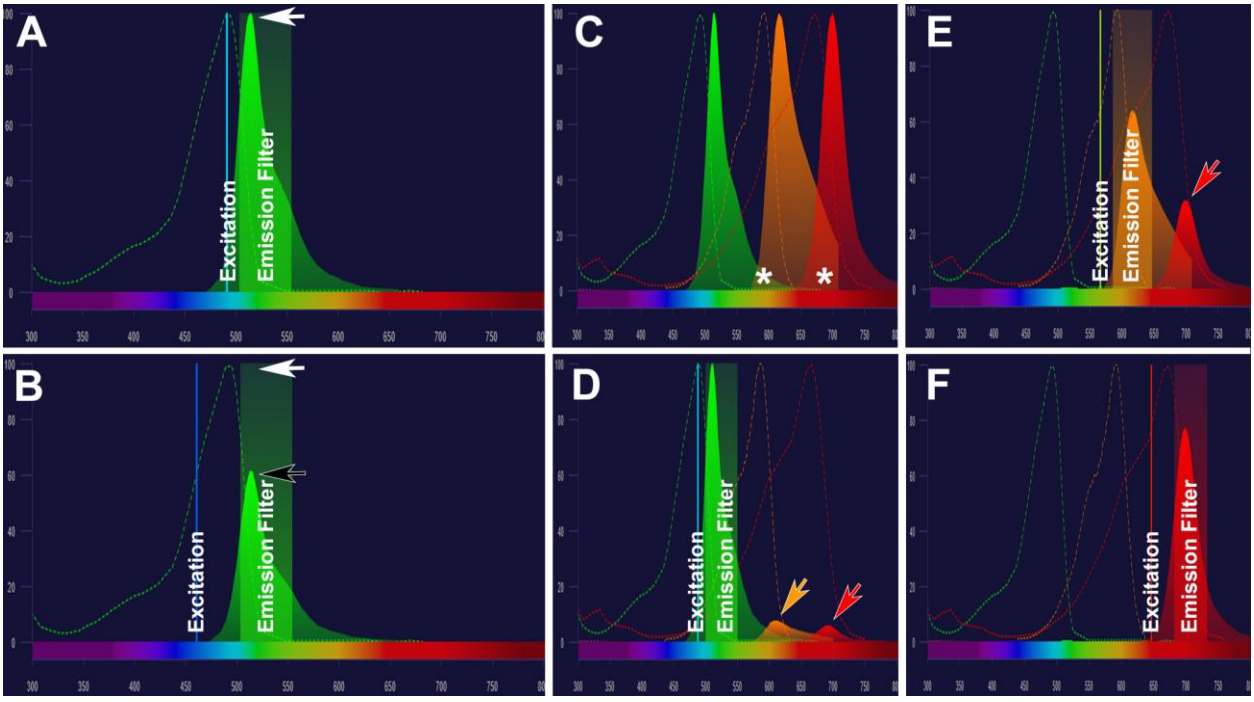

Figure 4: Fundamentals of excitation (dashed lines, unfilled curves) and emission spectra (solid lines, filled curves) and their relationship to microscope excitation (single vertical lines) and emission filters (thick vertical bars). (A) The fluorescence emission maximum from EGFP (white arrow) when excited with 488 nm laser (vertical cyan line) and collected with 525/50 (500-550 nm) bandpass emission filter (transparent green thick vertical bar). (B) With suboptimal 458 nm excitation of EGFP (compare white versus black arrow), there is an ~40% decrease in peak emission intensity compared to 488 nm laser excitation when using the same emission filter as (A). (C) When performing multicolor experiments, fluorophore selection (including potential autofluorescence) and imaging setup/strategy must be carefully considered to avoid detection of emission signal overlap due to crosstalk. Note emission spectra overlap portions (white asterisks) of the EGFP (green filled), mCherry (orange filled) and Alexa Fluor 660 (red filled) signals. (D) Imaging of one dye at a time with EGFP (488 nm excitation, 525/50 bandpass emission filter) still excites and collects mCherry (orange arrow) and Alexa Fluor 660 (red arrow) signals, but this sequential imaging limits crosstalk into the EGFP image. (E) Likewise, sequential imaging of mCherry (561 nm excitation, 610/60 bandpass emission filter) prevents excitation shorter wavelength

fluorophores (i.e., EGFP) and reduces Alexa Fluor 660 (red arrow) crosstalk in the mCherry image. (F) Finally, sequential imaging of Alexa Fluor 660 (640 nm excitation, 700/50 bandpass emission filter) prevents any lower wavelength fluorophore crosstalk into the image. Spectra created using ThermoScientific Fluorescence SpectraViewer (SpectraViewer 2024).

Figure 5

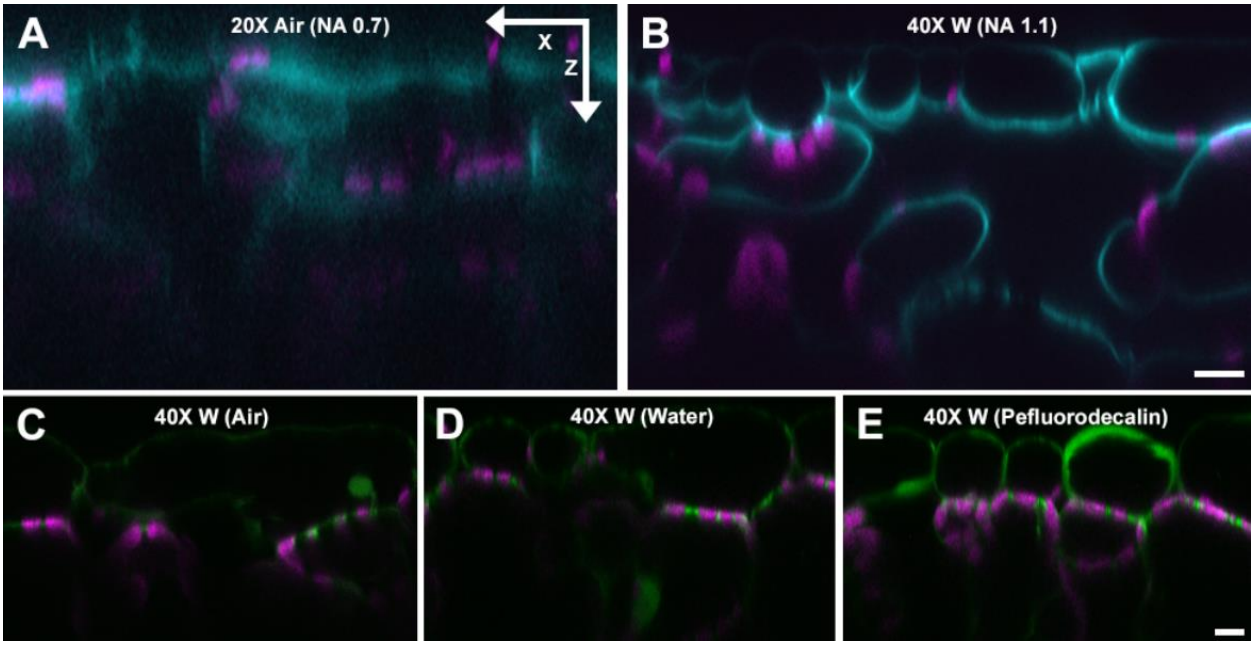

Figure 5. Comparison of objective lens and sample infiltration medium for live-cell imaging of *N. benthamiana* leaf epidermal and mesophyll cells. Single xz axis images of a tobacco leaf showed dramatically reduced image quality using a lower magnification/numerical aperture (A) 20X Air (NA 0.7) compared with a (B) 40X W (NA 1.1) objective lens. Scale Bar = 5 µm. Due to differences in spherical aberration, leaves that were mounted in water but not infiltrated to remove air spaces (C) 40X W (Air) exhibited reduced intensity and image quality, especially in deeper parts of the tissue, compared to water infiltrated leaves (D) 40X W (Water) or with best match of refractive index when using (E) Perfluorodecalin infiltrated leaves (40X W (Perfluorodecalin). Cell cytoplasm (cyan or green), Chlorophyll autofluorescence (magenta). Refractive Index of air = 1, water = 1.33, perfluorodecalin = 1.313. Scale bars = 10 µm.

Figure 6

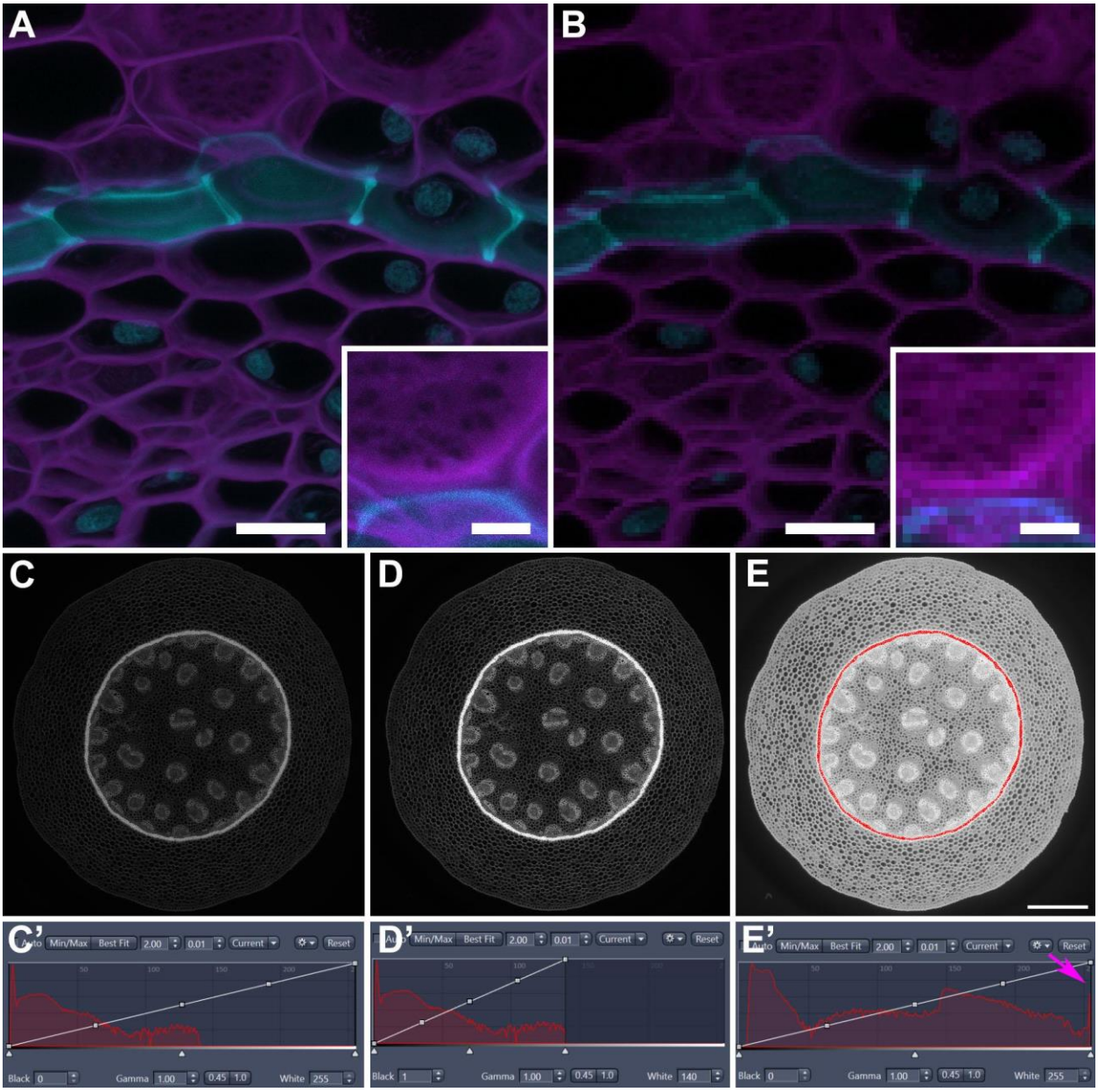

Figure 6. Pixel resolution and dynamic range on a test sample. (A) An image of an acridine orange stained Convallaria stem section acquired at an image pixel number (2048x2048) and size (57 nm) that met Nyquist sampling requirements and achieved the best possible resolution for a 40X Water (NA 1.1) objective lens. (B) A comparison of the same location as (A) with reduced image pixel number (128x128) and size (918 nm) that did not meet Nyquist sampling but was acquired ~250 times faster. (B) would be sufficient to identify nuclei and measure cell area or shape, but not fine detail of the image (compare

insets for magnified detail with/without Nyquist sampling conditions). Scale bars = 20 µm. Inset scale bars = 5 µm. (C) The dynamic range of an 8-bit image can be assessed by viewing its corresponding histogram (C') and the dynamic range optimized for viewing and display by selecting min/max (D and D'). It is essential to avoid (E) "clipping" the data (loss of information) by overexposure as evidenced with a range indicator to show any saturated pixels (red in E) or by reviewing the image histogram (E') which showed stacking of pixels at the extremes (magenta arrow). The Zeiss ZEN specific range indicator was applied in images C – E to show under (blue) and over saturated (red) pixels. Note: range indicator colors will vary depending on software/ vendor used. Scale bar = 500 µm.

Figure 7

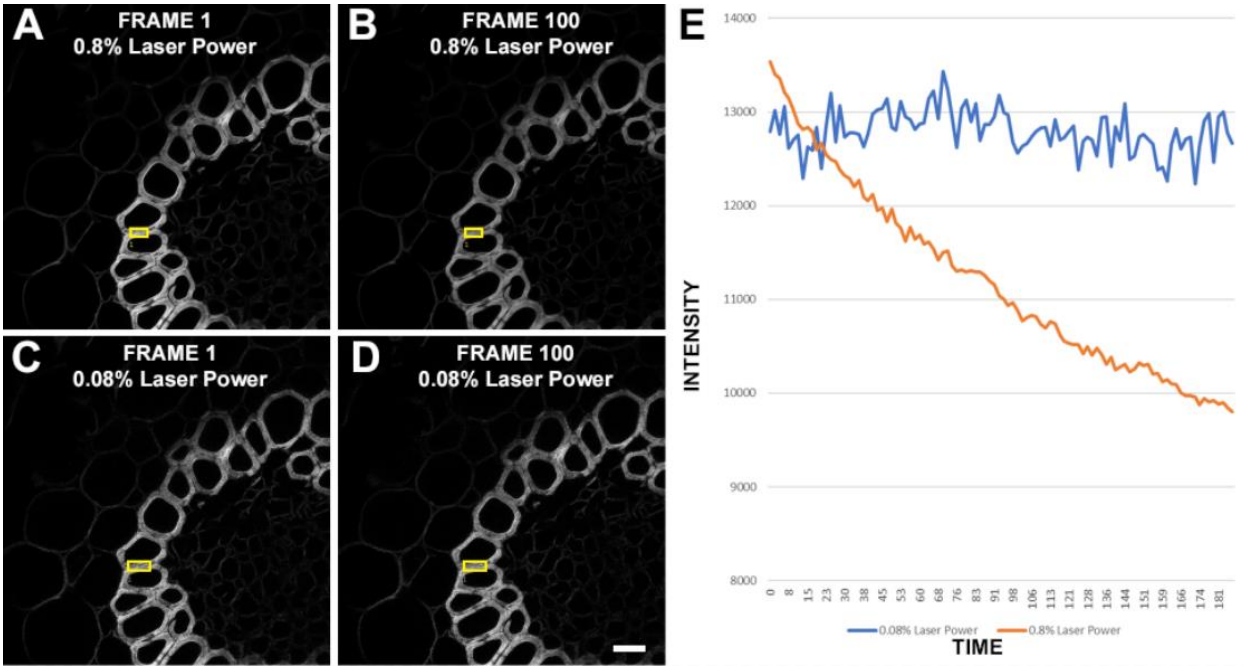

Figure 7. Effects of laser power on photobleaching. 100 frame time-lapse series of an acridine orange stained Convallaria stem section acquired over 185 seconds, at (A) FRAME 1 B) final FRAME 100 at 0.8% Laser Power (488 nm) showed lower signal intensity in FRAME 100 compared to FRAME 1 due to photobleaching. Decreasing the laser power by 10-fold (0.08% Laser Power) showed comparable signal intensity in Frame 1 (C) versus FRAME 100 (D). (E) Plotting the intensity over time in a region of the cell wall (yellow box) in this sample showed that while the 0.08% Laser Power (blue line) was noisier, it displayed minimal photobleaching compared to 0.8% Laser Power (orange line) where the signal decreased about 30% in this ~185 second time-lapse. Scale bar = 20 µm.

Figure 8

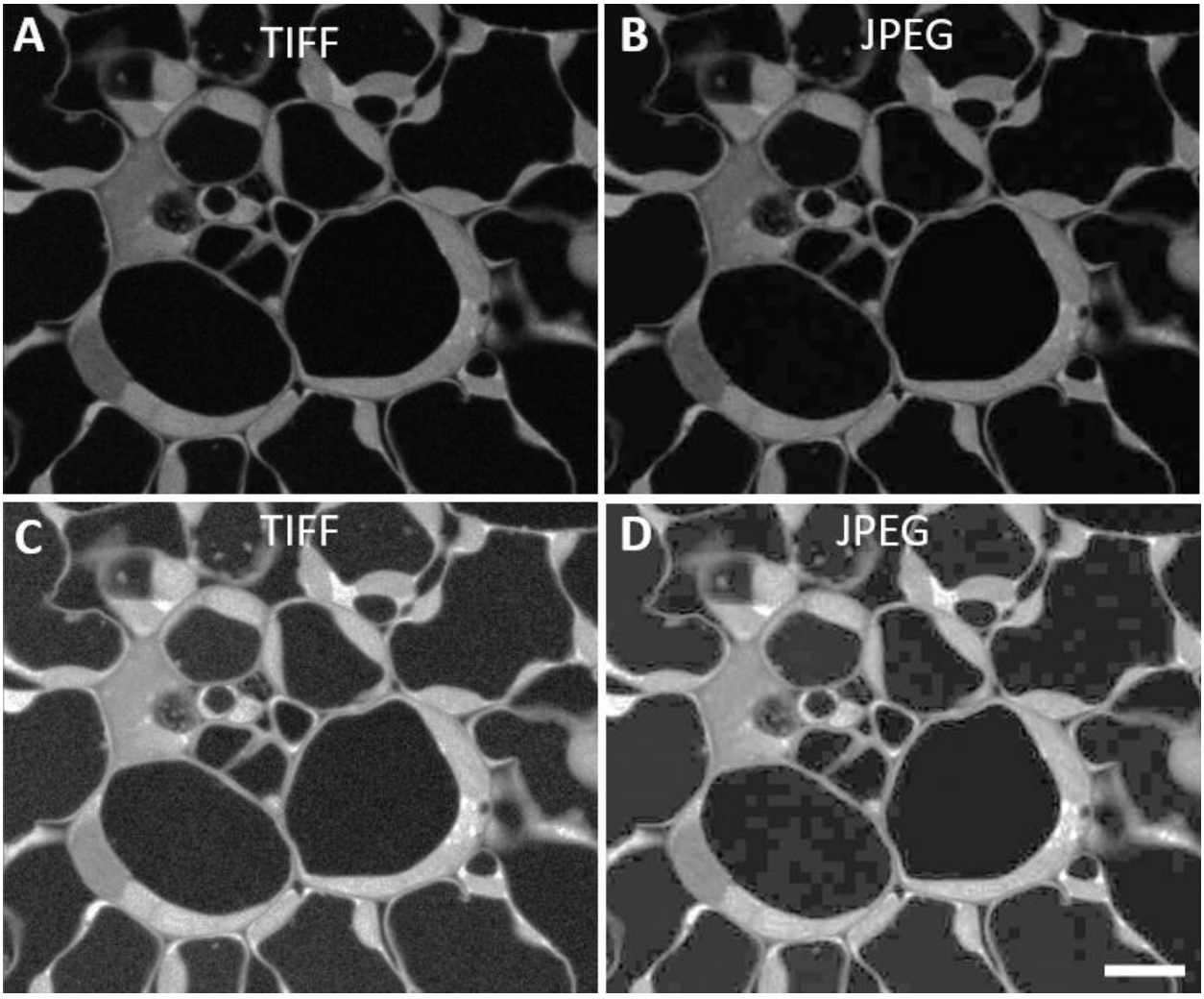

Figure 8. Image formats and lossless (TIFF) versus lossy (JPEG) compression. (A) A 1024x1024 pixel image of an acridine orange stained Convallaria stem section saved as TIFF compared to JPEG compression (B). (C) Increasing the image brightness of the TIFF image (A) showed fine texture in vacuoles and no detail loss. (D) Increasing the image brightness of the JPEG image (B) revealed numerous artifacts and edge effects from the altered/compressed pixels making this data impossible to reliably quantify. Scale bar = 20 µm.

Figure 9

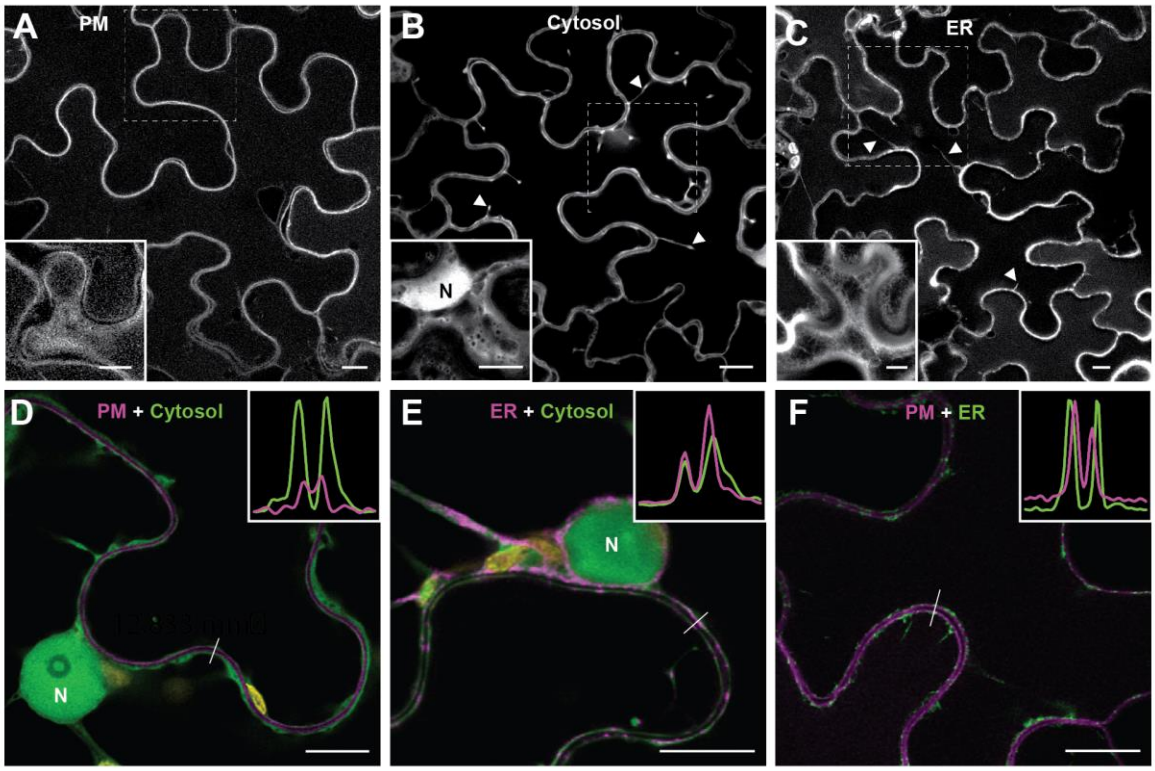

Figure 9. Distinguishing different membranes in plant cells. (A-C) Mid-plane view and insert of cortical view of *N. benthamiana* leaf epidermal cells transiently transformed with plasma membrane (PM) marker, PIP2A-mCherry (pm-RK; Nelson et al 2007))(A); cytosolic marker, untagged GFP (B), and the synthetic mCherry-tagged endoplasmic reticulum (ER) marker er-RB (Nelson et al 2007) (C). The main panels show a cell around its mid-point, while the insets show a region of the same cell but close to its cortex. The dotted lines mark the areas shown in inserts. Arrowheads indicate transvacuolar strands. (D-F) Border regions between *N. benthamiana* leaf epidermal cells transiently co-expressing markers for PM (pm-RK, magenta) plus cytosol (untagged GFP, green) (D), ER (er-RB, magenta) plus cytosol (untagged GFP, green) (E), and plasma membrane (pm-RK, magenta) plus ER (er-GB,green) (F). Chlorophyll autofluorescence is yellow. Inserts show line scan analyses for the white lines drawn in the main panels. The X-axis of the graph corresponds to the position along the line (the total line length is 4.2 µm, 3.5 µm, and 4.9 µm in D, E, and F, respectively), while the Y-axis shows the fluorescent intensity for both channels at each point along the line. Note the differences in the relative

position of the peaks from the two channels. All images were subjected to deconvolution using Olympus FluoView software. N, nucleus; Scare bars = 10 μm.

Supplementary Figure 1

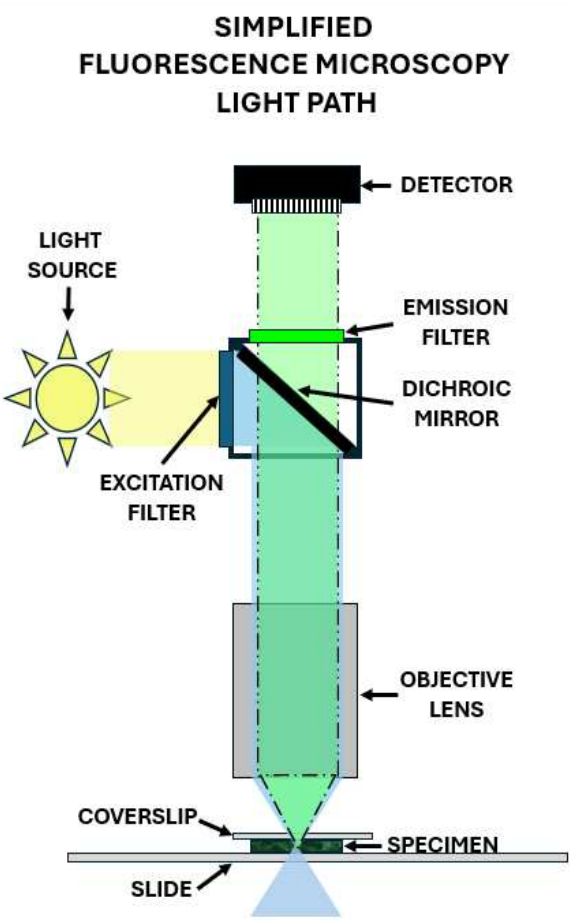

Supplementary Figure 1. A simplified upright fluorescence microscopy light path. The light source is directed through a dichroic filter cube which contains an excitation filter, a dichroic mirror, and an emission filter. The excitation filter is used to select the excitation wavelength and the dichroic mirror reflects the light through to the objective lens, which acts as a condenser, focusing the light into the specimen. Fluorescence emission signals will be generated at longer wavelengths which pass back through the objective lens and then are transmitted through the dichroic mirror and emission filter. The emission filter is used to define what wavelengths match the target signal (e.g., GFP) and the signal is collected by the detector (e.g. camera, photomultiplier tube or other).

Supplementary Figure 2

Supplementary Figure 2. Low-cost method of sample preparation of leaf tissue. (A) 6 mm biopsy punch, 10 ml syringe and parafilm strips. (B). C) Using proper PPE, use a 6 mm biopsy punch and rubber stopper behind the leaf to remove leaf disks (D). (E) Add or draw up water, buffer or buffer with stain into the syringe to desired level, remove the plunger (F), add leaf disks, replace plunger and while orienting the syringe with tip upward (H), carefully push out any trapped air. Note the leaf disk has a light coloration due to air within the mesophyll. While pressing at the syringe tip with an index finger to close off the

aperture, gently pull the syringe plunger to create a vacuum and note air bubbles coalescing on the leaf surface (I), release the index finger and the surrounding solution will enter the leaf, replacing the air spaces (J). Repeat the cycles a few times until the entire leaf darkens (K). (L) Using double-sided adhesive spaces, (M) mount onto a standard glass slide. (O) Add a small drop of water/buffer solution to the center of the well, (P) place the leaf disk onto the drop in desired orientation (e.g., adaxial/or abaxial facing up). To minimize air trapped between the coverslip and leaf surface, (Q) place a small drop of solution on a 22X30mm coverslip, quickly invert, (R) align and (S) place the coverslip onto the adhesive chamber and gently press along edges to seal. (T) Inspect to ensure minimal air bubbles between the tissue and the coverslip. Small bubbles adjacent to the leaf disk are acceptable if not interfering with leaf surface imaging.

Supplementary Figure 3

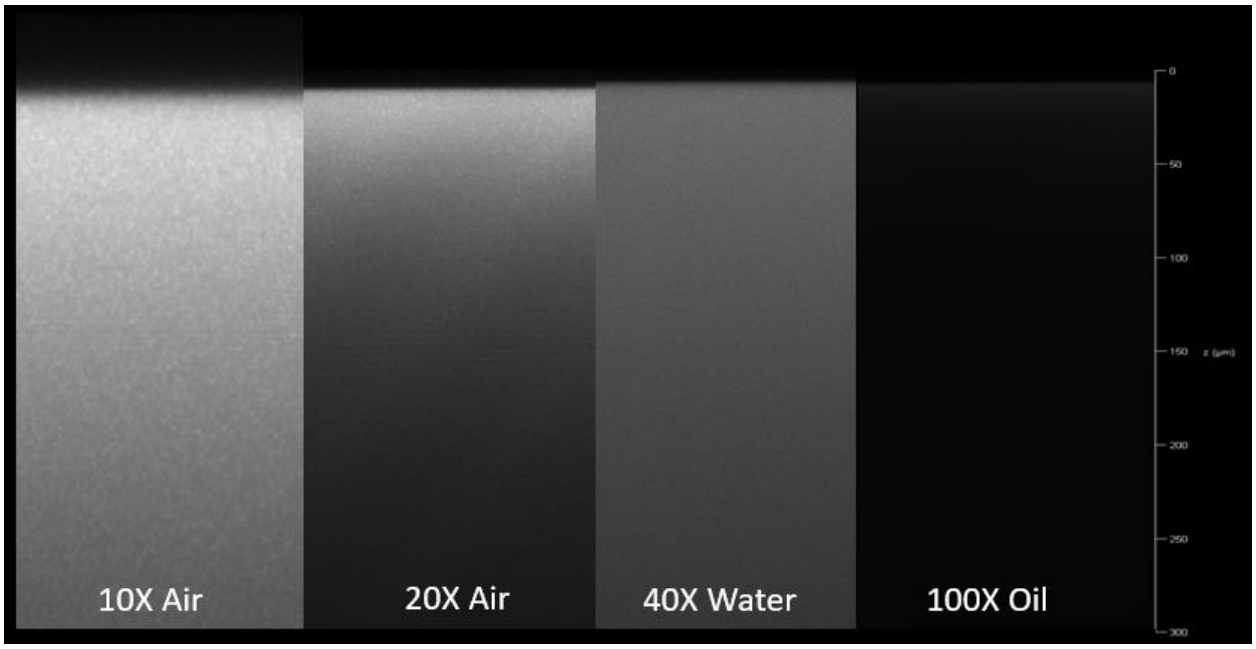

Supplementary Figure 3. Quantitative imaging of thick samples can be impacted by objective lens choice. This objective comparison showed XZ axis images that extended from the coverslip (top) to ~300 µm z-depth (bottom) of a FITC infiltrated agar slab with similar optical properties to living tissue. Each hash mark represents 50 µm. Signal Intensity using a low magnification/numerical aperture 10X Air (NA 0.3) or intermediate magnification/numerical aperture water immersion 40X Water (NA 1.1) was greater and more uniform with increased depth than the 20X Air (NA 0.70) or 100X Oil (NA 1.4) largely due to spherical aberration. However, the 100X NA 1.4 lens outperforms these other lenses in resolution when imaging very near the coverslip

Supplementary Figure 4

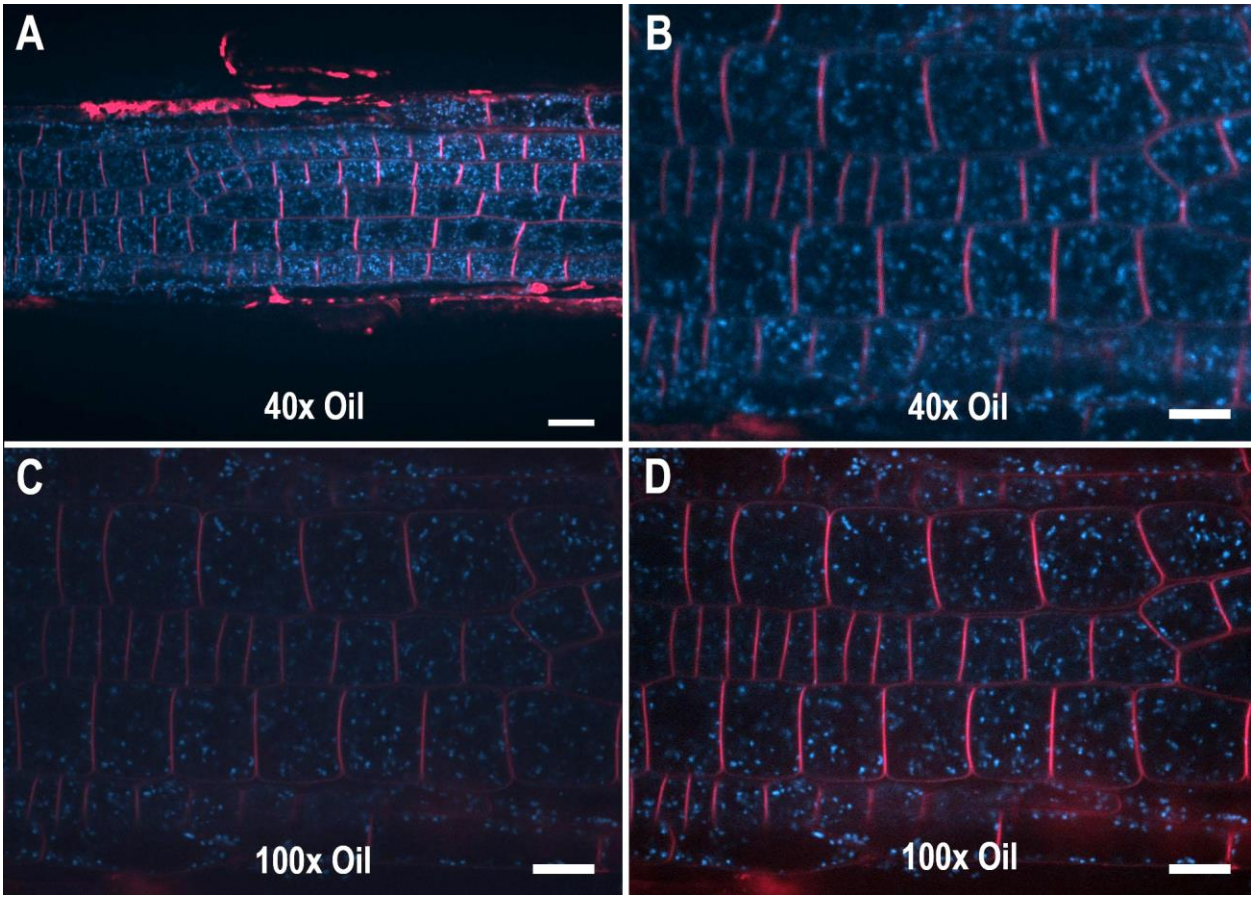

Supplementary Figure 4. 40X and 100X oil objective lens comparison of *A. thaliana* root division zone epidermal cells using spinning disk confocal microscopy. (A) Overview and (B) digital zoom image of *A. thaliana* root imaging of membrane stain, FM4-64 (magenta) and Syntaxin of Plants SYP61 CFP-SYP61 (cyan) collected with a 40x NA 1.3 oil immersion objective. (C) Under the same acquisition settings as (A) but using a 100X NA 1.49 oil immersion objective, a notable loss in signal strength (compare A & C) but rescaling of the histogram (D) showed an increase in contrast and cellular detail (resolution) of CFP-SYP61 vesicles. (A) Scale bar = 20 μm, (B-D) Scale bar = 10 μm.

Supplementary Figure 5

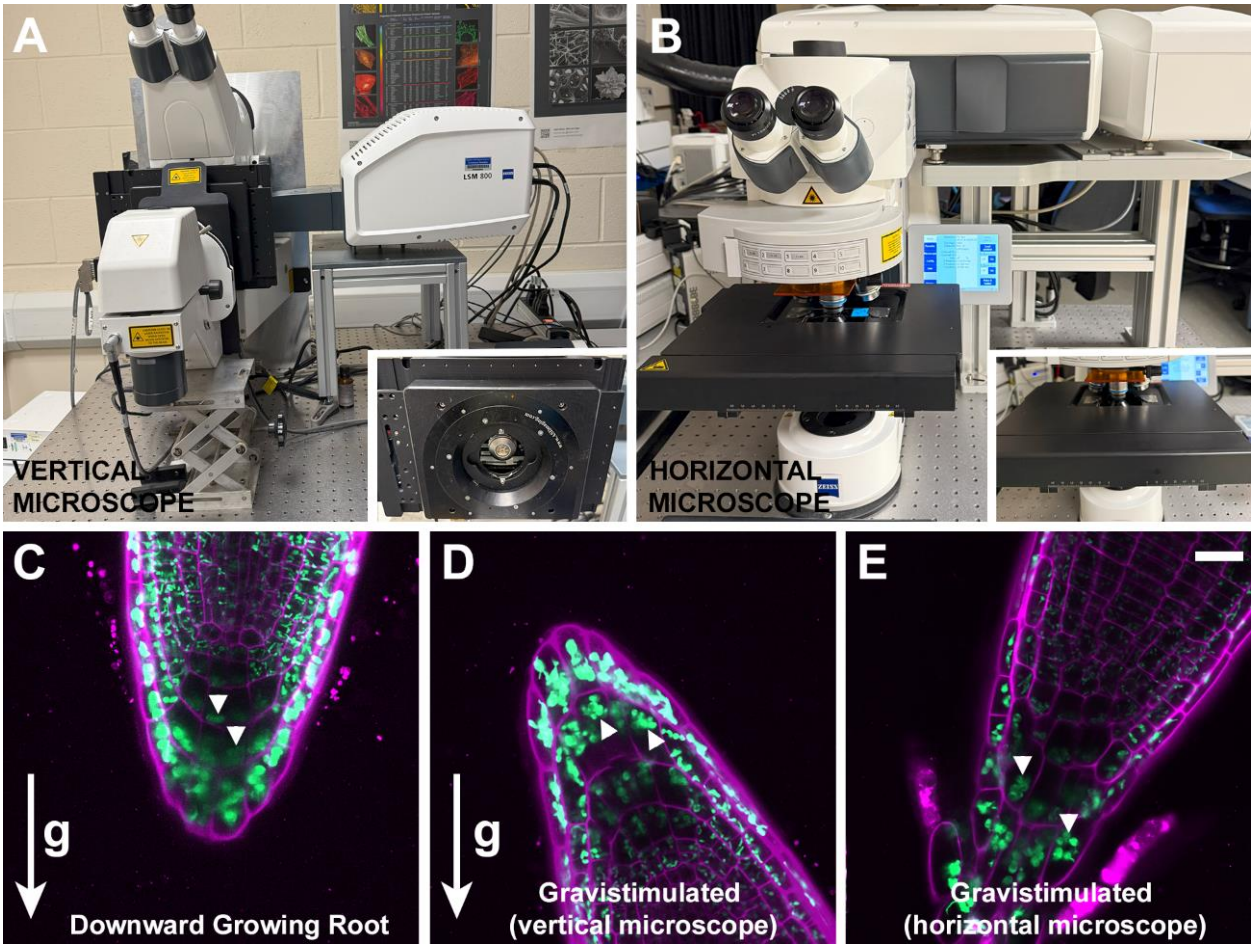

Supplementary Fig 5: Dynamics of gravi-dependent amyloplast sedimentation in Arabidopsis primary roots. (A) Overview of a vertically mounted Zeiss LSM800 confocal microscope compared to a horizontal stage microscope (B) used to image the Arabidopsis transgenic marker line (Pt-YK) expressing YFP tagged plastids counterstained with propidium iodide (magenta) for analysis of gravity-dependent statolith sedimentation. . (C) Dense starch filled amyloplasts (green) sediment towards the physical bottom of gravity sensing columella cells in Arabidopsis primary roots. (D) In gravistimulated roots, the sedimentation of these amyloplasts (indicated by white arrowheads) towards the new physical bottom of these cells can be clearly visualized when imaged with a vertical confocal microscope. (E) However, the dynamics of amyloplast sedimentation are lost when images are captured with a conventional horizontal microscope. Scale bar = 20 µm.